UNDERSTANDING PLUTONISM IN THREE DIMENSIONS:
FIELD AND GEOCHEMICAL RELATIONS ON THE SOUTHEAST FACE
OF EL CAPITAN, YOSEMITE NATIONAL PARK, CALIFORNIA

Roger Putnam

A thesis submitted to the faculty of the University of North Carolina at Chapel Hill in partial fulfillment of the requirements for the degree of Master of Science in the Department of Geological Sciences.

Chapel Hill
2013

Approved by:

Allen F. Glazner

Drew S. Coleman

Tamlin M. Pavelsky

ABSTRACT

ROGER PUTNAM: Understanding a plutonism in three dimensions: field and geochemical
relations on the southeast face of El Capitan, Yosemite Valley, California
(Under the direction of Allen F. Glazner)

Detailed mapping of the spatial extents of exposed rock units on the vertical southeast

face of El Capitan was completed to determine the chronology and geometry of

emplacement. Field relations display a complex intrusive history at the point of interaction

between two intrusive suites and two mafic dike swarms. Mapping revealed two sets of aplite

dikes with trace element compositions suggestive of derivation from intrusive suite of

Yosemite Valley or Buena Vista Crest magmas. Within the El Capitan and Taft Granites, 62

samples from multiple km-tall transects were analyzed for major- and trace-element

abundances. Texture analysis was completed on 78 scale photographs of El Capitan Granite.

No systemic variations in texture, mineralogy or chemistry were found in either the Taft or El

Capitan Granites. These observations are consistent with incremental pluton assembly and

are hard to reconcile with models for magma chambers that are envisioned as large,

convecting, fractionating bodies.

ACKGNOWLEDGMENTS

TABLE OF CONTENTS

LIST OF TABLES

Table

LIST OF FIGURES

Figure

LIST OF ABBREVIATIONS

a   annum

ISYV   intrusive suite of Yosemite Valley

ka   thousands of years/thousands of years before present

Ma   millions of years/millions of years before present

TIMS   thermal ionization mass spectrometer

TIS   Tuolumne Intrusive Suite

XRF   X-ray fluorescence

INTRODUCTION

Plutonic rocks are the principal rock type composing the earth's crust, yet much about their emplacement and evolution remains poorly understood. Traditional hypotheses have been dominated by the idea that plutons form by the rapid ascent of massive, largely liquid magma bodies into the crust (Daly, 1933; Buddington, 1959; Bateman, 1992; Miller and Paterson 1999). Such magma bodies could freeze in place or pause until a trigger, such as a fresh injection of magma, remobilizes them, causing large, silicic volcanic eruptions (Coombs and Gardner, 2001; Bachmann et al., 2002; Turner et al., 2010; Deering et al., 2011). The large shallow magma chambers envisaged in this model could then produce high- and intermediate-SiO$_2$ melts and zoned magma chambers via processes such as magma mixing and gravity-driven crystal/liquid fractionation (Reid et al., 1983; Bacon and Druitt, 1988; Verplanck et al., 1999; Bachl et al., 2001).

Crystal/liquid fractionation should produce both vertical and horizontal zonation in mineral abundances, whole-rock compositions, and trace-element signatures as mafic minerals crystallize and residual melt rises and moves to the center of the pluton (Baker and McBirney, 1985). *In situ* crystal-liquid fractionation of a single intrusion has often been invoked as the mechanism of formation of zoned plutons including the Tuolumne Intrusive Suite, California (Bateman and Chappell, 1979), the Palisade Crest Intrusive Suite, California (Sawka et al., 1990), the Organ Needle Pluton, New Mexico (Verplanck et al., 1999) and the plutons of the Colorado River extensional corridor, Nevada (Bachl et al., 2001; Miller and

Miller, 2002). Vertical profiles of ignimbrites frequently display compositional patterns suggesting that their parental magma chambers were zoned and were emptied from the top down during eruption (Bacon and Druitt, 1988). The studies focused on plutons, are based on data collected from sub-vertical transects (Sawka et al., 1990; Verplanck et al., 1999).

For a variety of geochemical, structural, and seismic reasons, these traditional emplacement models have been questioned (Coleman et al., 2004; Glazner et al., 2004). These authors proposed that many plutons are amalgamated from numerous smaller intrusive events over long periods of time. The temperature at which this occurs remains high for millions of years, allowing these increments to anneal, creating a superficially uniform body (Bartley et al., 2008; Gray et al., 2008; Michel et al., 2008; Davis et al., 2011). Because crystal settling and chemical diffusion in silicic, high-viscosity melts occur too slowly at emplacement levels to permit differentiation by gravitational crystal/liquid fractionation (Eichelberger et al., 2000; Clemens et al., 2010), the compositional heterogeneity of many intrusive bodies are inferred to be a signature of changes in the lower crustal source of the magma, and not a result of *in situ* processes (Tappa et al., 2011; Coleman et al., 2012).

These two models ascribe very different roles for crystal/liquid fractionation during pluton emplacement. Therefore, a true vertical geochemical profile of a pluton provides an excellent test of these contrasting hypotheses. El Capitan in Yosemite Valley, California is a ~1 km tall, distinctively clean, continuous, vertical exposure that is crossed by over 100 named climbing routes. Two major intrusive suites and two mafic dike swarms intersect on this face. This exposure offers a unique opportunity to study interactions between intrusive units and to test hypotheses regarding the mechanisms of pluton emplacement.

2

GEOLOGIC BACKGROUND

El Capitan is ~1 km^3 Cretaceous granite monolith exposed in the west-central portion

of the Sierra Nevada batholith and is composed of members of the intrusive suite of

Yosemite Valley (ISYV) and the intrusive suite of Buena Vista Crest (Figure 1; Reid et al.,

1983; Bateman, 1992; Ratajeski et al., 2001). Most mapping of El Capitan has focused on

outcrops along the base and on the summit dome and on optical reconnaissance (Calkins,

1930; Bateman 1992; Peck, 2002). Mafic dike swarms cropping out on the face were used to

study magma mixing processes by Reid et al. (1983), Ratajeski et al. (2001), and Nelson et

al. (2012). A detailed map of the summit was made as a part of a study of the ISYV (Figure

2; Ratajeski et al., 2001), and a portion of the southeast face was mapped in order to study

the genesis of a prehistoric rock avalanche (Stock and Uhrhammer, 2010).

The Intrusive Suite of Yosemite Valley

Numerous units of the ISYV are exposed on the summit and face of El Capitan. This

suite of plutons is interpreted to have been emplaced in a continental-arc environment 105-95

Ma (Stern et al., 1981; Bateman, 1992). To the west, the ISYV intrudes Paleozoic

metasedimentary rocks and granodioritic units of the ~115 Ma Fine Gold Intrusive Suite,

(Bateman, 1992). To the east, the ISYV is intruded by the Late Cretaceous Tuolumne Intrusive Suite (TIS; Bateman, 1992), which was emplaced from 95-85 Ma (Figure 1; Coleman et al., 2004; Memeti et al. 2010).
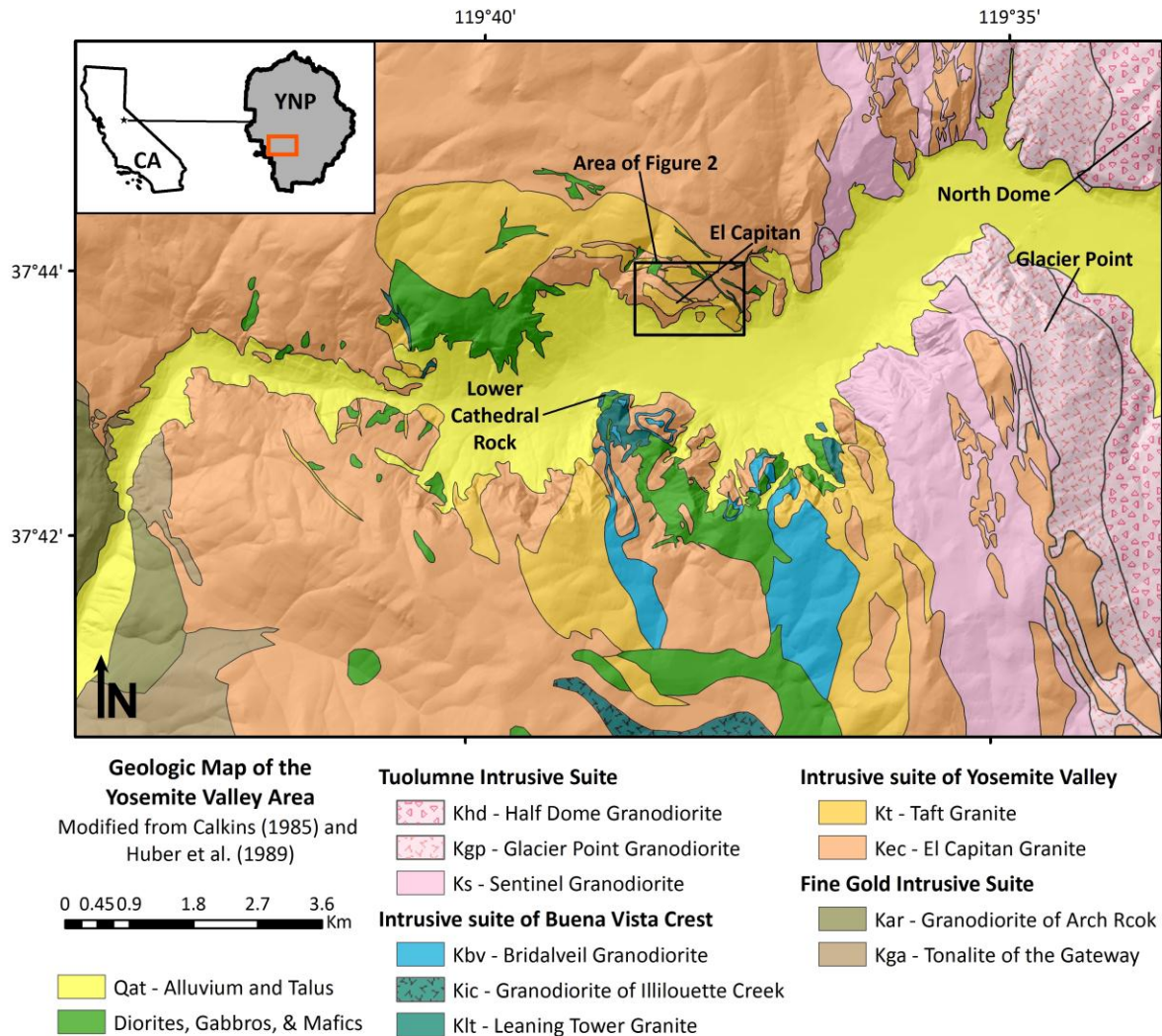
Figure 1 Geologic map of the Yosemite Valley area. Modified from Calkins et al. (1985) and Huber et al. (2002). Diorite, gabbro, and all other mafic units colored green, regardless of age or intrusive suite association.
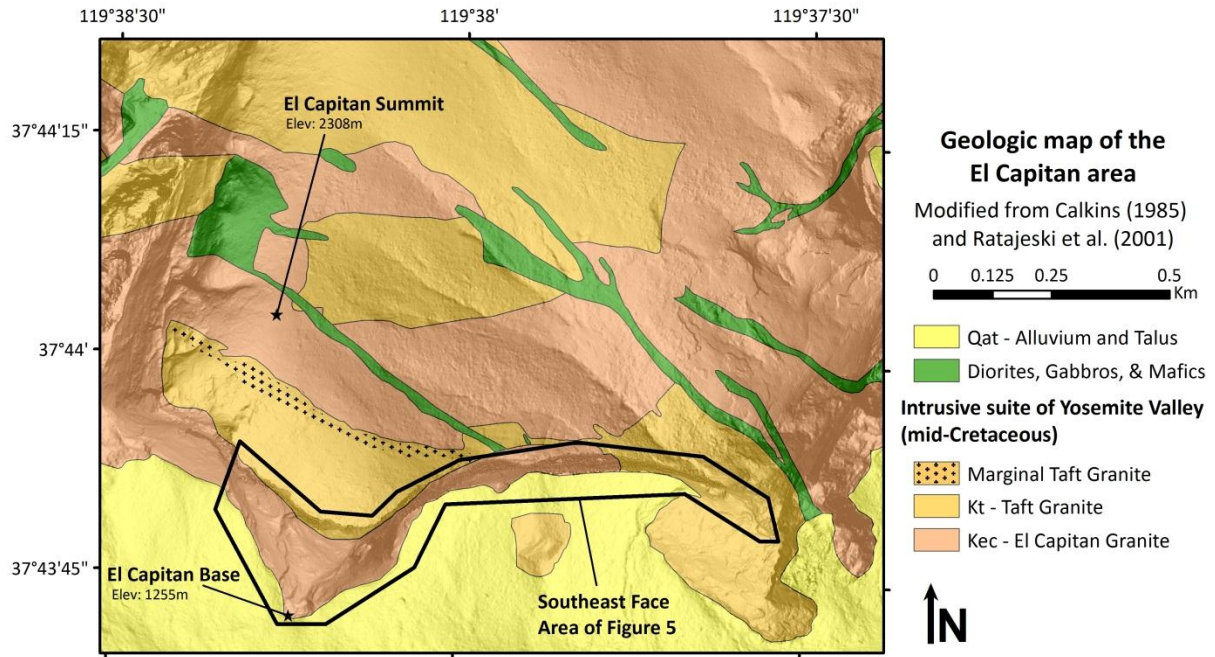
Figure 2 Geologic map of the El Capitan summit area modified from Calkins et al. (1985) and Ratajeski et al (2001).

Granites

The El Capitan Granite is the dominant unit exposed on the southeast face of El Capitan and was the first unit to be emplaced (Ratajeski et al., 2001). The main body of the pluton is 30 km long and 5 km wide and is a principal member of the ISYV (Bateman, 1992). It is a K-feldspar porphyry (1-2 cm) with biotite as the principal mafic mineral (Appendix 1). Recent U-Pb dating of the El Capitan Granite suggests an age of 105.43 ± 0.95 Ma (Ingalls, 2011). Isotope ratios (Nd and Sr) and experimental data suggest that the granite was generated by partial melting of relatively young mafic sources, perhaps hydrous gabbroic rocks in the lower crust (Ratajeski et al., 2001, 2005) with a contribution from recycled crust (Nelson et al., 2012).

The Taft Granite intrudes and is more leucocratic than the El Capitan Granite. It is fine-grained, equiangular, and is dominantly composed of quartz, plagioclase, and alkali feldspar with minor amounts of biotite. The El Capitan and Taft Granites overlap on all major and trace element trends although the Taft is richer in SiO_2 overall (Bateman, 1992). The Taft Granite has proven difficult to date: Stern et al. (1981) obtained a discordant U-Pb age of 95 Ma, but Ratajeski et al. (2001) found that Taft zircons, like those of the El Capitan, plot near concordia at 102-105 Ma. It is hypothesized that the Taft represents either partial melting of El Capitan Granite, a smaller-degree of partial melt of the same source, or a partial melt of a more silicic source than the El Capitan Granite (Ratajeski et al., 2001).

Mafic units

The El Capitan and Taft Granites are both cut by a series of compositionally diverse, biotite-rich, hornblende-poor, moderately dipping intrusions of dioritic to granodioritic rock previously referred to as pre-North America dikes (Ratajeski et al., 2001) and herein called dikes of the Oceans after their abundance in the outcrops east and west of the North America feature (Figure 3). These dikes thermally and chemically interacted with the host rock and contain partially reacted xenoliths of other plutonic rocks up to ~15 m across (Reid et al., 1983; Ratajeski et al., 2001).

A steeply south-dipping tonalitic unit crops out in the center of the *Nose* route. This unit was mapped as diorite separating the El Capitan and Taft Granites by Calkins (1985) and Peck (2002) and was mapped by Ratajeski et al (2001) as a marginal facies of the Taft Granite (Figure 2). Because it is compositionally similar to the biotite-rich, hornblende-poor dikes of the Oceans, it was interpreted as coeval mafic material that was mixed with the Taft

6

Granite during emplacement (Ratajeski et al., 2001). Herein it is referred to as tonalite of the

Gray Bands.
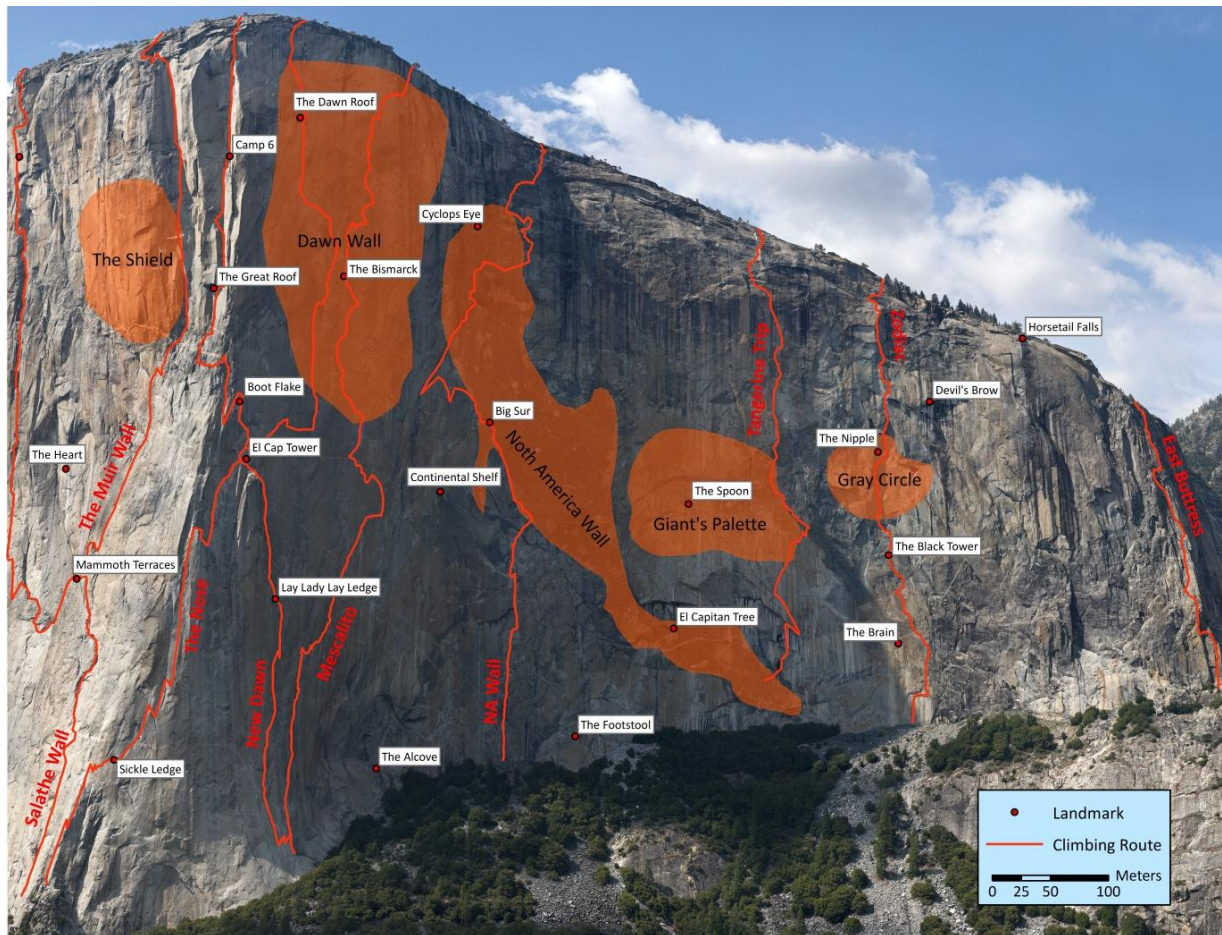
Figure 3 The southeast face of El Capitan with notable locations and climbing routes indicated. The *Nose* route travels along the curving arête separating the sunlit and shaded parts of the cliff. The "North America Wall" is the concave section of wall to the right of the *Nose*, marked by a mafic dike in the shape of North America.

The diorite of North America is a series of steeply dipping mafic dikes that derives its

name from the resemblance of its exposure to the continent of North America (Figure 3). It

displays high compositional and textural variability, but is largely Al-rich hornblende gabbro

and diorite (Ratajeski et al., 2001). Precise dating of the diorite of North America has proven

difficult, but it is spatially associated with the Taft Granite and they are interpreted to be

coeval because the contacts of the diorite with the Taft Granite are diffuse and often grade into schlieren (Ratajeski et al., 2001).

Intrusive Suite of Buena Vista Crest

The intrusive suite of Buena Vista Crest mostly crops out south of the intrusive suite of Yosemite Valley and, in some areas, intrudes it. Bateman (1992) recognized this suite as normally zoned, comprised of the following successively younger inward map units: the Granodiorite of Illilouette Creek and Leaning Tower Granite, the granodiorite of Ostrander Lakes, the granodiorite of Breeze Lake, the Bridalveil Granodiorite, and the granite of Chilnualna Lake. The Granodiorite of Ostrander Lake was discordantly dated at ~112 and 107 Ma (Stern et al., 1981) and the Granodiorite of Illilouette Creek was dated at 99±1 Ma (Tobisch et at., 1995).

Reconnaissance mapping (Bryan Law, pers. comm., 2011) indicated that Leaning Tower Granite crops out on El Capitan. It is a medium-gray, medium-grained rock with distinctive biotite and hornblende clusters ~10 mm in diameter. Bateman (1992) mapped it as a marginal facies to the intrusive suite of Buena Vista Crest and inferred that it was coeval with the Granodiorite of Illilouette Creek. The type locality for this unit is located on the south side of Yosemite Valley in the Cathedral Rocks area, and Calkins (1985) did not map it in the vicinity of El Capitan.

METHODS

Mapping

Mapping of the southeast face of El Capitan at a ~1:500 scale was conducted using a number of datasets and techniques: 1) remote sensing using LiDAR point cloud and return strength data; high-resolution gigapixel photographs of the southeast face taken by xRez Studios (www.xrez.com) and as part of this investigation; photographs of rock texture taken by rock climbers as they ascended the cliff (Figure 4); and high-resolution photographs taken of the cliff face from El Capitan Bridge by climbing photographer Tom Evans; 2) direct examination by rappelling the *Prophet* and the *Nose* and climbing the *Muir Wall*, *New Dawn*, *Zodiac*, *Freeblast*, *East Buttress* and lower half of the *North America Wall* (Figure 3). We constructed gigapixel photos in May 2012 using a Gigapan robotic camera mount with a Nikon D5000 SLR and a 300 mm lens. Typical pixel size for these photos was ~2 cm.

The map was initially made using ESRI ArcGis software. In ArcMap, contact lines of different units were manually digitized over a gigapixel image of the southeast face. These polygons were assigned rock types using scale photographs taken by climbers. Where contacts were obscured by shadows, lichen, surface encrustation, or photo stitching errors, Tom Evans photographs were examined because they were taken during a variety of lighting conditions and from different vantage points that often had better perspective than the gigapixel photographs.

Figure 4 Example of mapping methods. (B) and (C) are the area around the 7th belay on the climbing route *Tangerine Trip*, which is indicated by the circled 7 on both images. Note the climbers around the belay for scale. The scale photograph taken at this location is displayed in (A). (B) is a high resolution image with the contacts of units digitized and (C) displays the assigned units. Pink is El Capitan Granite (Kec), light green is dikes of the Oceans (KdO), and dark green is the diorite of North America (Kd). Light yellow lines are aplite dikes and the dark thick red line is the path of the climbing route.

Texture Analysis

Scale photographs taken by climbers on the southeast face presented a unique opportunity to study changes in rock texture in the vertical dimension. Using the Exelis ENVI image processing package, mineral types were classified using simple color thresholds in 78 scale photographs taken over much of the extent of the El Capitan Granite. Images were classified in accordance to the distribution of biotite and hornblende (black-brown), feldspars (white-pink) and quartz (gray). Only photographs of fresh faces with no shadows were selected for this analysis. For each mineral type, contiguous regions representing individual crystals, defined using a 4-connect neighborhood, were automatically identified. Crystals the size of 1 pixel were ignored. From these classifications, the relative mineral group abundances and mean crystal sizes were calculated.

10

Sample Collection

Samples were collected from the base, summit, and face of El Capitan and from the base of Lower Cathedral Rock on the south side of Yosemite Valley. Samples from the face were primarily collected from belay stances on climbing routes from sites that had no impact on the climbing route. Specific climbing routes were selected for sampling because they passed through large stretches of single units. Samples collected from El Capitan include El Capitan Granite, Taft Granite, tonalite of the Gray Bands, Leaning Tower Granite, and aplites (Appendix 1). Samples collected from Lower Cathedral Rock include Leaning Tower Granite and Bridalveil Granodiorite. Aplite samples were collected along the walls of the valley from El Capitan east to North Dome (Figure 1).

Whole-Rock and Trace-Element Geochemistry

Whole-rock and trace-element analyses of granite were performed using wavelength dispersive X-ray fluorescence (XRF) at the University of North Carolina at Chapel Hill on a Rigaku Supermini XRF spectrometer. Fresh portions of each sample were broken up with a rock hammer, crushed using a jaw-crusher, and powdered in a ceramic shatter box. For major-element analysis, the powders were dried for a minimum of 8 hours at 100°C. Loss on ignition for each sample was determined by heating ~2 grams of rock powder to 950°C for 1.5 hours. Ignited sample $(0.9000 \pm .0010$ g) and 64.7% lithium tetraborate, 35.3% lithium metaborate, 0.5% lithium bromide flux $(8.1000 \pm 0.0010$ g) was melted in a Pt crucible and fused into a glass bead. Trace element analyses were also performed with XRF using paraffin pressed powder disks. Unignited samples $(6.0000 \pm 0.0005$ g) were combined with paraffin

powder (0.6000 ± 0.0005 g), mixed in a ball mill, and pressed into a disc in an Al mold with a hydraulic press.

Geochronology

A number of samples were selected for geochronology by both laser ablation and thermal ionization mass spectrometry. All samples were broken down using a jaw crusher and a disc mill. Zircons were separated using standard density (water table and heavy liquids) and magnetic techniques. Samples selected for laser ablation dating include LC-01 (Leaning Tower Granite), LC-02 (Bridalveil Granodiorite), RF-01 (El Capitan Granite from the western margin of the unit), ECS-01 (Taft Granite), and YOS-104 (diorite of North America). Grains (50-100) representative of the population's size and morphology were separated from each sample, mounted in epoxy and polished using standard polishing techniques. They were dated by laser-ablation multicollector inductively coupled plasma mass spectrometry using the analytical techniques described by Kylander-Clark et al. (2013).

A sample of Leaning Tower Granite (LC-01) from the base of Lower Cathedral Rock, the type locality of the unit, was selected for U-Pb dating. Zircon grains were thermally annealed at 900°C for 48 hours and were chemically abraded in 29M HF for 16 hours at 220°C to remove mineral inclusions and zones affected by radiation damage that are subject to Pb-loss (Mattinson 2005). Fractions were spiked with a ^{205}Pb-^{233}U-^{236}U tracer (Parrish and Krogh 1987) and dissolved in 29M HF following a procedure modified after Krogh (1973) and Parrish (1987). Anion exchange (HCl) column chromatography was used to isolate U and Pb from the dissolved solution.

Analyses of U and Pb were completed using a VG Sector 54 thermal ionization mass spectrometer at the University of North Carolina at Chapel Hill. Uranium was run on single Re filaments either as a metal, after loading in graphite and H_3PO_4, or as an oxide, after loading in silica gel. Lead was loaded in silica gel on single, zone-refined Re filaments. Both U and Pb were analyzed in single-collector peak-switching mode using a Daly ion-counting system. Data processing and age calculations were completed using the applications Tripoli and U-Pb_Redux developed as part of the EARTHTIME initiative (Bowring et al., 2011; McLean et al., 2011). Decay constants used were $^{238}U = 1.55125 \times 10^{-10}$ a^{-1} and $^{235}U = 9.8485 \times 10^{-10}$ a^{-1} (Steiger and Jäger 1977).

Corrections for initial Th/U disequilibrium (Mattinson 1973; Schmitz and Bowring 2001) were made using U-Pb_Redux. An assumed magmatic Th/U ratio of 4 was used based on an average Th/U ratio of all granodiorites in the Sierra Nevada batholith according to data in the NAVDAT database (www.navdat.org). The difference between an uncorrected $^{206}Pb/^{238}U$ weighted mean age and an age that has been corrected for a magmatic Th/U ratio of 3.7 is approximately 95 ka in these samples.
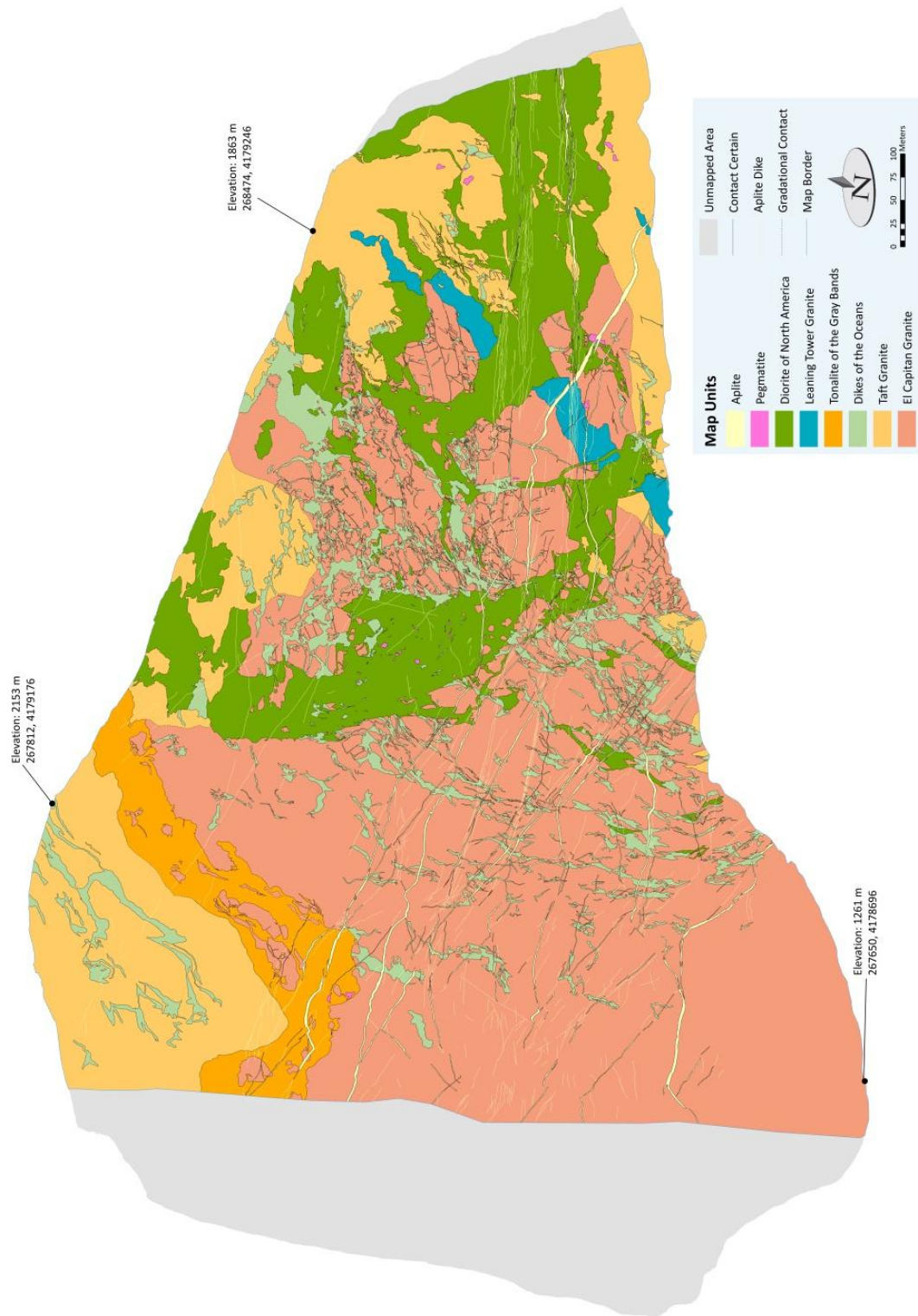
Figure 5 Geologic map of the southeast face of El Capitan. The vertical distance on the left hand edge of the mapped area is nearly 1000 m.

14

RESULTS

Field Relations

The new mapping (Figure 5) reveals field relations that help to resolve an intrusive history previously obscured by problematic geochronology and physical inaccessibility. The first intrusion, the El Capitan Granite, is distinctly homogenous in outcrop, with little obvious modal layering. On the southeast face, magmatic fabric is rare, and if present, poorly developed. Mafic enclaves are uncommon (less than 10^{-4} area fraction) and typically small (<10 cm diameter).

The Taft Granite primarily crops out in a wedge that extends ~250 m deep centered on the upper third of the *Nose* climbing route as mapped by Calkins (1985), and in a large block centered on the *East Buttress* climbing route that extends west along the base to El Capitan Tree (Figure 3). From El Capitan Tree, the Taft Granite intermittently crops out along the base west to the Alcove in dikes up to 0.5 m thick that cut the El Capitan Granite. These dikes have sharp to gradational margins and tend to be more leucocratic than typical Taft. Where the Taft contacts the El Capitan Granite on the face (such as 40 m up the route *Zodiac*), the contact is gradational with little diking. Much of the unit is modally layered and sometimes contains marginally more mafic bands up to 10 m thick. There is no apparent pattern to the orientation or width of these features.

The next several intrusive episodes following intrusion of the Taft Granite were interpreted by prior work to be were roughly contemporaneous (Reid et al., 1983; Ratajeski

et al., 2001). However, crosscutting relations approximately 600 m up the *Nose* route reveal that the first of these was the dikes of the Oceans. Dikes of the Oceans strike east and dip ~40˚ south on the upper part of the *Nose*, and dip much more steeply on other parts of the cliff. They commonly display dextral sense-of-separation indicators, especially on the western part of the face. Contacts of the dikes of the Oceans with the Taft and El Capitan Granites tend to be sharp to gradational over ~0.25 m. Contacts of the dikes of the Oceans with all other units are sharp, and the dikes commonly contain abundant enclaves of the diorite of North America in mafic pods and swarms (Figure 6), indicating that the two intrusive episodes were diachronous.

The tonalite of the Gray Bands crops out below the Taft Granite between the *Salathe Wall* and *Mescalito* and dips steeply to the southwest. It is in sharp contact with the El Capitan and Taft Granites and contains angular xenoliths of El Capitan Granite up to ~20 m across (Figure 7). Locally, the intrusion appears to be a composite of 0.5-1 m thick interfingered dikes.

The Leaning Tower Granite principally crops out at the bottom of the cliff below El Cap Tree and runs in a large, diagonal, *en echelon* band up to the east and past the Gray Circle. This band is ~30 m wide at the base of the cliff and gradually tapers out to the east. One smaller band crops out about 75 m east of *Zodiac* and pinches out up and to the east as does the large band. The Leaning Tower Granite's contacts are typically sharp although sometimes gradational over ~5 m.

Figure 6 A telephoto photograph of a climber's camp just above "The Spoon" on the climbing route *Iron Hawk*. The rectangular hanging ledge is approximately 2 m long. The host El Capitan Granite was intruded by many mafic dikes of the Oceans, the largest of which is choked with enclaves of the diorite of North America. The lower left is a comparatively recent rock-fall scar and has not grown lichen or oxidized yet. Photo courtesy of Tom Evans.
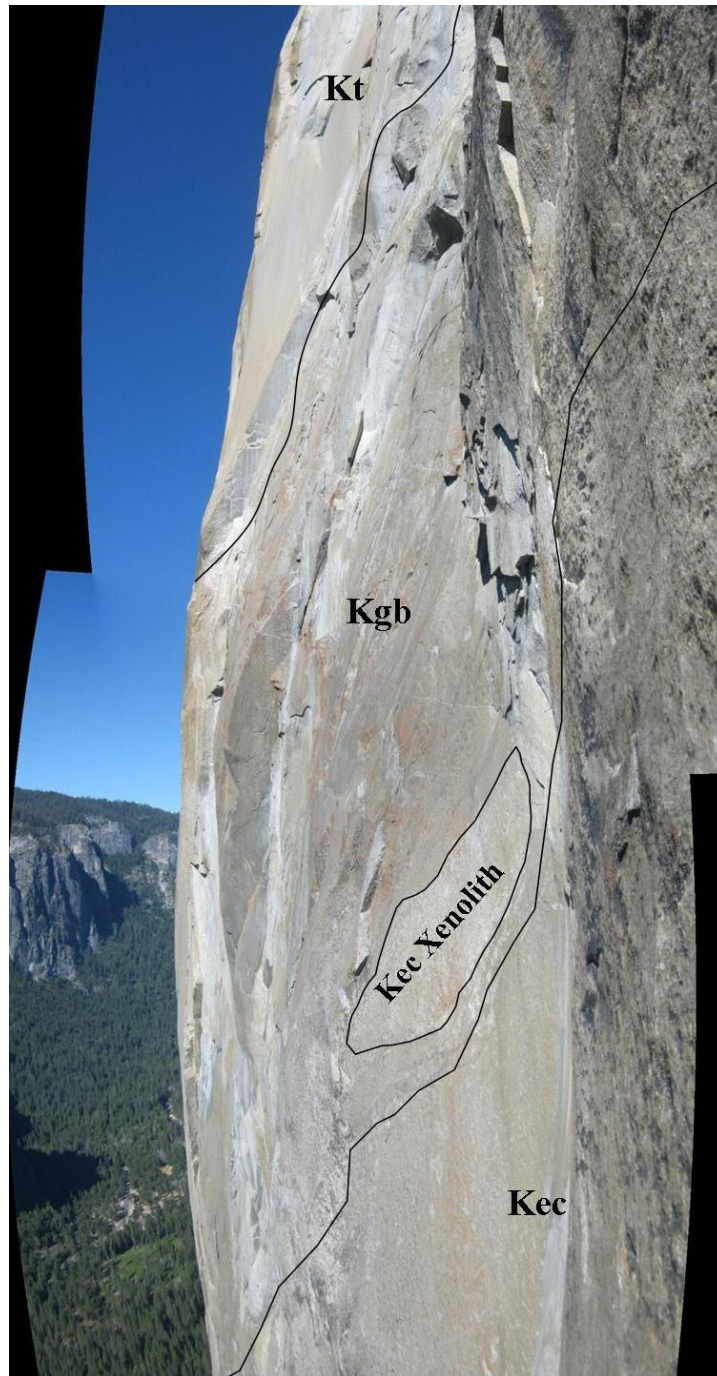
Figure 7 A panorama taken from ~750 m up *New Dawn* looking west across the tonalite of the Gray Bands (Kgb). Above the tonalite is the Taft granite (Kt) and below it is the El Capitan Granite (Kec). Note the large (~10 m across the minor axis) xenolith of El Capitan Granite and the sharp contact between the tonalite of the Gray Bands and the surrounding units. Also note the composite nature of the unit, especially around the "Kgb" symbol.

The diorite of North America intruded in three ~50 m thick composite dikes that strike southeast and dip nearly vertically. They crop out on the southeast face in North America, around the Gray Circle, and just east of the *East Buttress* (Figure 3). Because these dikes dip so steeply, they superficially resemble large masses from Yosemite Valley floor. The diorite of North America captured xenoliths of host rock up to ~20 m across. Its contacts with all other units are sharp or gradational over ~1 m.

Two series of aplite dikes cut the southeast face. First-series dikes are 0.5 - 3 m thick and dip steeply to the northeast. They appear to be composite and commonly contain 2 – 10 cm thick pegmatite bands. The second series are 0.1 – 0.2 m in thickness and are subhorizontal. The horizontal series crops out along the northern walls of the valley and cuts every unit older than the Tuolumne Intrusive Suite. In a few locations, the second series clearly cuts the first, suggesting separate emplacement events (Figure 8A). The first series is deformed, displaying inconsistent sense-of-separation indicators, whereas the second series is largely undeformed.

Xenoliths of host metasedimentary or metavolcanic rock are conspicuously absent from the southeast face of El Capitan; none were found in this study, nor by any of the climbers engaged in the study. The nearest mapped xenoliths of wall rocks to El Capitan are located near Sentinel Dome, ~5 km to the southeast

Figure 8 (A) Photograph showing the first (large, steeper dipping) series of aplites being cut by the smaller subhorizontal set. The aplites are hosted in Leaning Tower Granite on the upper left and El Capitan Granite on the lower right. This location is approximately 100 m up and left of "The Brain" (see Figure 4). The large dike is ~2m across. Photo courtesy of Derek Ferguson. (B) Y vs. Sr for aplites from El Capitan, the intrusive suite of Yosemite Valley, and the Tuolumne Intrusive Suite. Data are drawn from this study and from Glazner et al. (2008) (C) Map of all of the aplites collected in Yosemite Valley. Each symbol is proportionally sized for the amount of Y in the sample and color coded for the intrusive suite it is hosted in.

Petrography and Geochemistry

Petrographic characteristics of the ISYV were described by Calkins (1930), Pabst (1938), Smith (1967), Bateman et al. (1984), and Ratajeski et al. (2001) (Appendix 1). Major and trace element analyses of various units are presented by Bateman et al. (1984), Ratajeski et al. (2001), and Nelson et al. (2012). Our sampling and analysis focused on the felsic units to evaluate evidence for vertical variations in composition.

Sixty-two samples analyzed in this study range from 49 to 78 wt% SiO_2 but are essentially bimodal, with mafic rocks ranging from 49 to 57 wt%, granitic rocks ranging from 66 to 78 wt %, and only one sample of tonalite of the Gray Bands in the gap (Figure 9). The El Capitan and Taft Granites overlap in composition although the Taft is generally higher in SiO_2 (Bateman et al., 1984; Ratajeski et al., 2001). On most plots the tonalite of the Gray Bands continues the linear trends defined by the Taft and El Capitan Granites to lower SiO_2 concentrations, although it tends to be more compositionally diverse.

Textural and mineralogical data from the Leaning Tower Granite cropping out on El Capitan confirm its assignment to this unit as described by Bateman (1992). The Leaning Tower Granite has proportionally more hornblende, biotite, and plagioclase than the principal silicic units on El Capitan. Myrmekite occurs along plagioclase-K-feldspar boundaries and, similar to most granitoids in the Yosemite Valley area, biotite is moderately chloritized. Accessory minerals are dominantly magnetite, zircon, and titanite, with rarer apatite and epidote. Magnetite, zircon, and titanite tend to be spatially associated with biotite. The samples from the newly recognized outcrops on El Capitan geochemically cluster with samples taken from the type locality on the south side of Yosemite Valley. Leaning Tower Granite samples range from 68.3 – 70.1 wt % SiO_2 and are distinctively poorer in
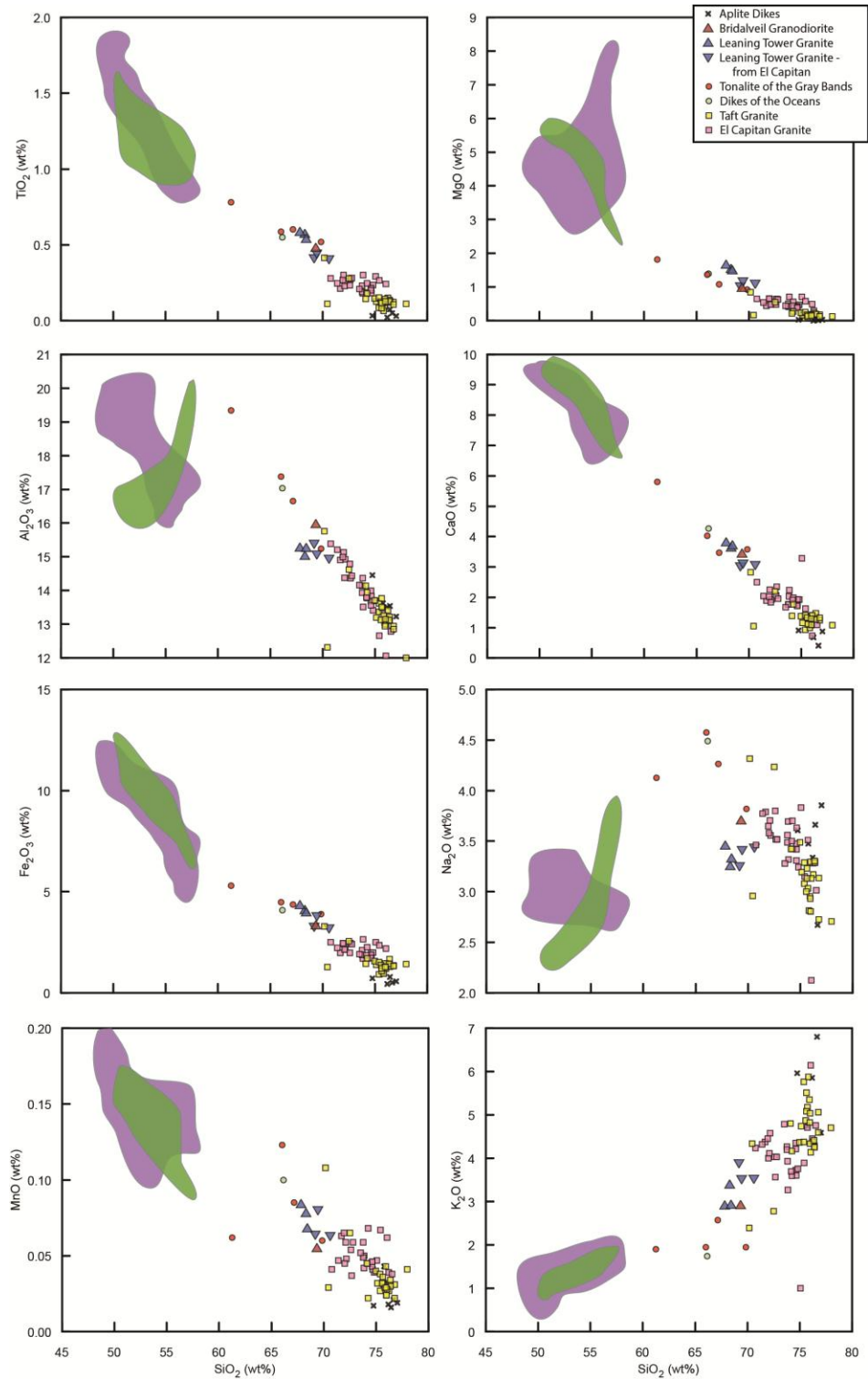
Figure 9 Major element variation diagrams. The green field is diorite of North America and the purple is the diorite of the Rockslides drawn from Ratajeski et al. (2001) and Nelson et al. (2012).

Al and Na than the rock of the ISYV (Figure 9). The samples taken from El Capitan are more mafic than the samples taken from the unit's type locality, with slightly more Ca, Mg, and Ti. Nevertheless, we interpret these as the same unit because they plot together for major element abundances and possess the same distinctive texture and mineralogy.

Both the dipping and the horizontal aplite dike series are quartz and K-feldspar rich and also contain trace amounts of garnet and muscovite. Garnet occurs locally in dense aggregations of mm-sized crystals, often in association with graphic texture within the dike as a whole. Both series typically contain ~76 wt% SiO_2 compared with 75 and 74 wt % SiO_2 for the Taft and El Capitan Granites respectively. They overlap on many other major-element trends as well (Figure 9). Despite the presence of garnet and muscovite, they are essentially metaluminous; molar $Al_2O_3/[CaO+K_2O+Na_2O]$ averages 1.03.

Vertical Patterns

There are no apparent patterns in major element composition with increasing elevation within individual units (Figure 10). Even when limited to the area of the cliff with the least evidence for felsic-mafic interaction, there are still no trends with increasing elevation (Figure 11). Texture analysis revealed no pattern in the mean crystal size or relative abundance of ferromagnesian (biotite and hornblende) minerals with increasing elevation (Figure 12). A similar analysis was performed for feldspar and no pattern can be observed. However, the feldspar analysis is less robust because it is impossible to distinguish between plagioclase and K-feldspar by color signatures alone.
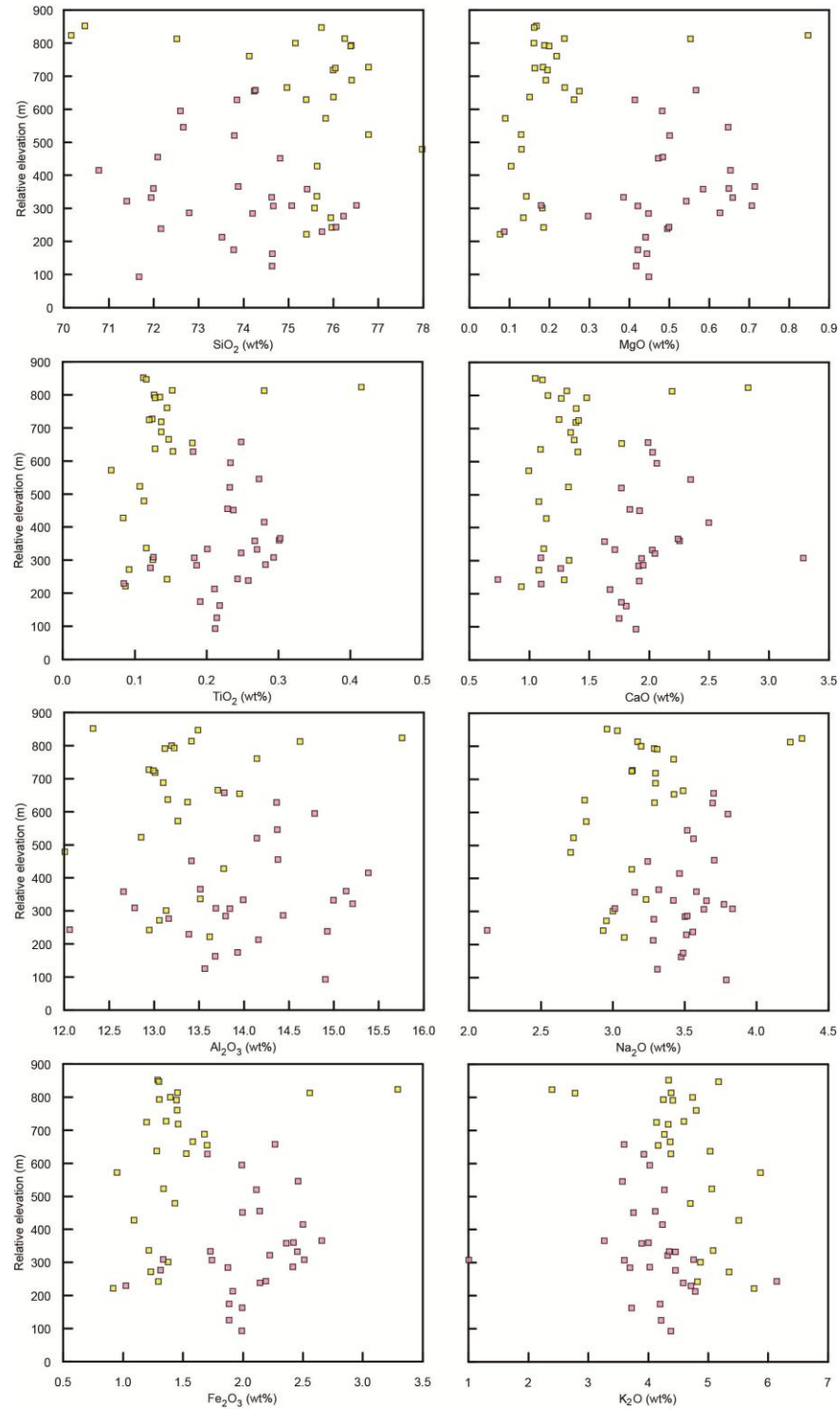
Figure 10 Major element variations plotted against the relative elevation from which the sample was collected. Relative elevation refers to the sampling location's elevation above the lowest exposed part of the southeast face, at the toe of the Nose. Pink squares are samples of El Capitan Granite and yellow squares are samples of Taft Granite.

24
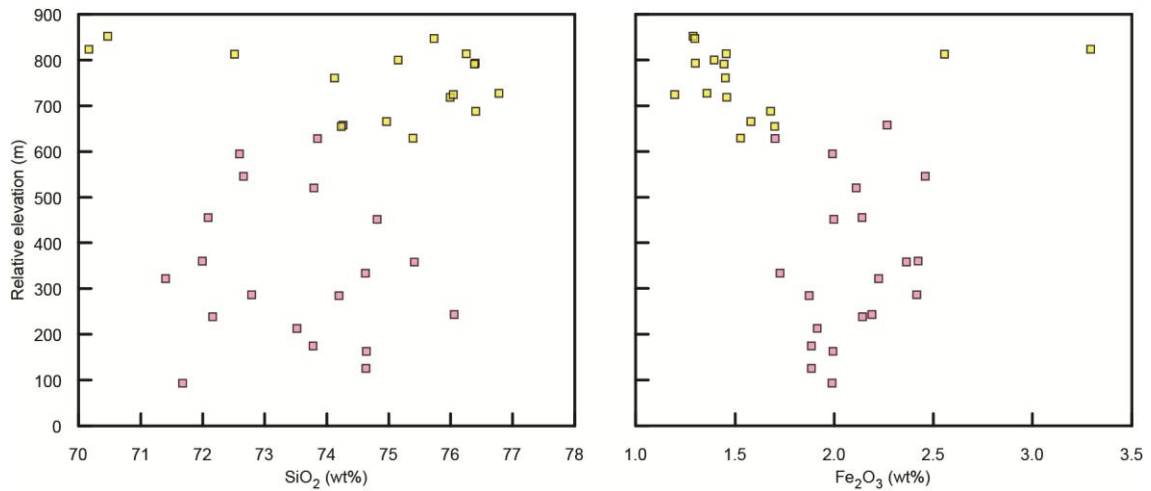
Figure 11 SiO$_2$ and Fe$_2$O$_3^{t}$ vs. relative elevation for samples taken from the *Nose*, *Muir Wall*, and *New Dawn* climbing routes. These routes are located on the part of the southeast face that is the tallest and has the least mafic-felsic interaction.
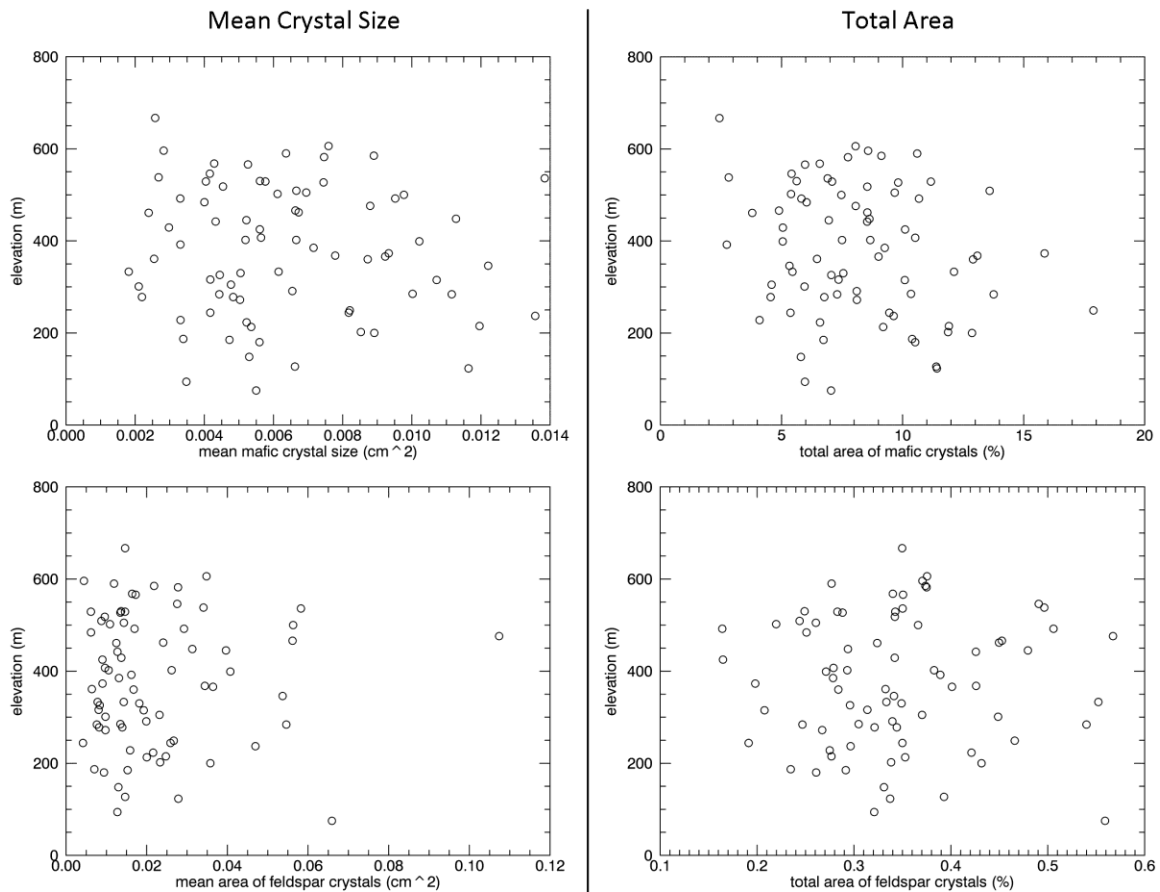
Figure 12 Plots of mafic mineral and feldspar size and abundance vs. relative elevation derived from scale photographs.

Geochronology

Sample LC-01 of the Leaning Tower Granite yielded a concordant weighted mean age by U-Pb TIMS of 104.05 ± 0.11 Ma (MSWD = 0.4; 4 fractions). A single fraction was discarded that was clearly inherited, plotting on concordia at 105.60 ± 0.13 Ma (Figure 13; Table 1).

U-Pb laser ablation data are summarized in Table 2. Two samples of the El Capitan Granite give mean ages of 106.6 ± 0.8 Ma (summit) and 105.6 ± 0.5 Ma. (Cookie Slide, near the west entrance of Yosemite Valley); a third, from the westernmost outcrops of the granite, near El Portal, gives a much older age of 116.4 ± 2.3 Ma. The Taft Granite sample has a bimodal age distribution, perhaps due to the presence of monazite. The monazite grains were recognized because of their high levels of Th and were discarded for the data reduction; remaining zircon points yield a mean age of 106.6 ± 1.1 Ma A sample of the diorite of North America yielded an age of 103.3 ± 0.6 Ma, and samples of Leaning Tower Granite and Bridalveil Granodiorite from the ISBVC yielded similar ages of 102.7± 2.5 Ma and 103.4 ±0.5 Ma respectively.
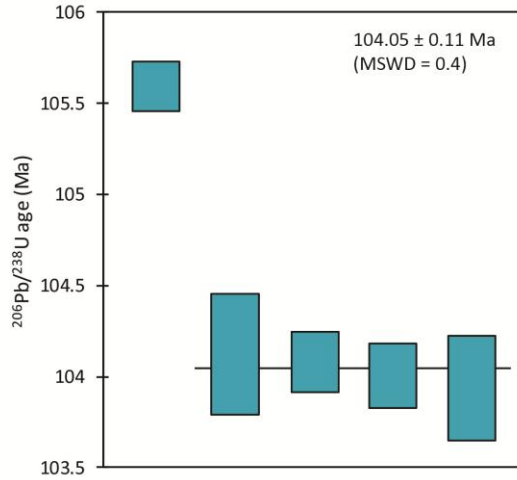
Figure 13 Summary of ^{206}Pb/^{238}U TIMS ages for sample LC-01. Data for all ages are concordant within analytical uncertainty. One fraction, LC-01 F3, has a distinctively older age that is the same as that is interpreted as being inherited from an older part of the magma system.

TABLE 1: ZIRCON TIMS AGE DATA FROM THE LEANING TOWER GRANITE

Sample fraction	U (ppm)	Pb* (pg)[a]	Th[b] U	^{206}Pb[c] ^{204}Pb	^{206}Pb[d] ^{238}U	Error (%)	^{207}Pb[d] ^{235}U	Error (%)	^{207}Pb[d] ^{206}Pb	Error (%)	^{206}Pb ^{238}U	^{207}Pb ^{235}U	^{207}Pb ^{206}Pb	Corr. coef.	Total[f] common Pb (pg)
F-1	545	10	0.51	259	0.0162691	0.32	0.1068419	4.58	0.0476295	4.38	104.13	103.07	78.8	0.640	2.6
F-2	924	17	0.45	429	0.0162506	0.17	0.1081699	2.62	0.0482765	2.50	104.01	104.29	110.7	0.704	2.6
F-3	596	39	0.41	931	0.0165007	0.13	0.1093568	1.19	0.0480663	1.12	105.60	105.38	100.4	0.521	2.7
F-4	3120	43	0.58	600	0.0162649	0.16	0.1079798	1.87	0.0481493	1.78	104.10	104.12	104.5	0.605	4.4
F-7	287	9	0.47	309	0.0162416	0.28	0.1084449	3.86	0.0484260	3.68	103.95	104.54	118.0	0.672	1.9

[a] Total mass of radiogenic Pb.

[b] Th contents calculated from radiogenic ^{208}Pb and the ^{207}Pb/^{206}Pb date of the sample, assuming concordance between U-Th and Pb systems.

[c] Measured ratio corrected for fractionation and spike contribution only.

[d] Measured ratios corrected for fractionation, tracer and blank.

[e] Th corrected isotopic dates calculated using the decay constants λ_{238} = 1.55125 x 10^{-10} and λ_{235} = 9.8485 x 10^{-10} (Jaffey et al. 1971), assuming Th/Umagma = 4.

[f] Total mass of common Pb.

Table 1 Summary of U-Pb dates obtained by thermal ionization mass spectrometry from sample LC-01 of Leaning Tower Granite.

TABLE 2. SUMMARY OF LASER ABLATION DATA

Sample	Rock type*	Location description†	Age (Ma)	error (Ma)	MSWD	Sample size
LC-01	Klt	Float at the base of the west side of the north face of Lower Cathedral Rock	102.7	2.5	47	36
LC-02	Kbv	Float at the base of the west side of the north face of Lower Cathedral Rock	103.4	0.5	1.1	36
YOS-104	Kd	Float at the base of the east side of North America wall sampled by Ratajeski (2001)	103.3	0.6	3.19	40
RF-01	Kec	In the town of El Portal, above Rancheria Flat (252762E, 4174384N)	116.4	2.3	11.3	34
ECS-276	Kec	Summit of El Capitan, sampled by Ingalls (2011)	106.6	0.8	3.19	40
CS720-5	Kec	Cookie slide, sampled by Ingalls (2011)	105.6	0.5	6.1	66
ECS-01	Kt	Slab ~200 m south of the start of Zodiac, (268449E 4179041N)	106.6	1.1	3.1	14

* Summary of abbreviations: Klt (Leaning Tower Granite), Kbv (Bridalveil Granodiorite), Kd (diorite of North America), Kec (El Capitan Granite), Kt (Taft Granite)

†Coordinates age given in UTM NAD 1983 zone 11N

Table 2 Summary of U-Pb dates obtained by multicollector inductively coupled plasma mass spectrometry.

DISCUSSION

Intrusive dynamics

The mapping effort produced the first (to our knowledge) effort to comprehensively map the vertical dimension of a granitic system at this scale. It reveals a complex and distinct intrusive history involving eight distinct intrusive episodes, many of which are diachronous. The cross-cutting relations and nature of contacts revealed by mapping simplify this history.

Contacts between the El Capitan and Taft Granites are typically gradational over ~0.25-1 m, whereas contacts between these granites and all other units are typically sharp. If gradational contacts are an indication of intrusion into a thermally active system, then our mapping and geochemistry agrees with Ratajeski et al.'s (2001) interpretation of the Taft Granite being generated from a partial melt of the same source as the El Capitan Granite and emplaced at the same approximate time. The complicated U-Pb systematics of the Taft Granite zircons do not resolve the chronology of emplacement. However, because dikes of Taft cut the El Capitan, as for example between the Alcove and the Footstool and at Taft Point, it must at least be younger locally, however small that age difference is.

Conversely, contacts between the dikes of the Oceans, the tonalite of the Gray Bands, and the Leaning Tower Granite with the units they intrude are sharp. This suggests that the system into which they were intruding was at low enough temperatures to prevent significant mixing.

Ratajeski et al. (2001) noted that the contacts between the diorite of North America and the Taft Granite tend to be diffuse and grade into schlieren on the summit, and interpreted these relations to indicate cogenesis. However, on the face of El Capitan the contact is typically quite sharp, which is consistent with the geochronology, which found phases of Taft Granite that are over 3 Ma older than the diorite of North America. The diffuse contacts observed by Ratajeski et al. (2001) could be the result of localized partial melting rather than cogenesis.

This field relation is the only sign of significant partial melting caused by the intrusion of a mafic unit. Perhaps this is because the diorite of North America is more voluminous than the other late-stage intrusive events and thus may have generated higher local temperatures at the time of intrusion. This higher thermal flux could have caused significant localized partial melting in the highly silicic Taft Granite, but not in the other, less silicic units into which it intruded.

Given the spatial relation of the dikes of the Oceans and the diorite of North America, and that the diorite of North America often intrudes as pillows, it is possible that the diorite of North America intruded along the rheological weaknesses provided by the still thermally active, perhaps higher melt-fraction dikes of the Oceans. This field relation has been observed in other exposures of silicic plutons (Wiebe and Collins., 1998; Leuthold et at., 2012).

Timing

Most of the units that crop out on El Capitan have been difficult to date by U-Pb TIMS, due to inherited grains, Pb loss, and less well-developed analytical methods (Stern et

al., 1981; Ratajeski et al., 2001). This problematic geochronology is partially resolved by our laser ablation and U-Pb TIMS data.

The El Capitan and Taft Granites are distinctly older than all of the other intrusive rocks in the El Capitan area and were emplaced around 106 Ma. The Leaning Tower Granite is younger than the dominant silicic units at 104.05 which is within uncertainty of the laser date of 102.7 ± 2.5 Ma. The diorite of North America is the same age as the Leaning Tower Granite within uncertainty (104 ± 0.3 Ma and 103.3 ± 0.6 Ma, respectively). This suggests that the El Capitan and Taft Granites were intruded about 1 m.y. before the other units, confirming observed field relations.

Previous geochronology on the El Capitan Granite was performed under the paradigm of traditional pluton emplacement, typically on samples taken from the central-eastern portion of the pluton (Stern et al., 1981; Ratajeski et al., 2001). We analyzed samples spanning a broader geographic area, including a sample from the far western boundary of the unit, ~15 m from the contact with Jurassic metasedimentary rocks. These analyses span ~10 m.y. in age. Although the sample set is small, it raises the possibility that El Capitan Granite may have had a prolonged duration of emplacement. This is surprising given that ages within individual Sierran plutons often range over 1-3 Ma (Coleman et al., 2004; Davis et al., 2011), which is longer than many plutons around the world. Either the El Capitan Granite was assembled over an unusually long time span or the map units of the intrusive suite of Yosemite Valley are more complicated than prior mapping suggests.

Taft Granite

The Taft Granite has been difficult to date. Stern et al. (1981) obtained a discordant U-Pb age of 95 Ma, but Ratajeski et al. (2001) found that Taft zircons, like those of the El Capitan, are ca. 102–105 Ma. This age range is significantly restricted by our TIMS date on the Leaning Tower Granite. Because the Leaning Tower Granite clearly cuts the Taft Granite, it must be the younger unit, which limits the age of the Taft to between the age of the El Capitan and Leaning Tower Granites (105.7 – 104.1 Ma in this area; Table 2)

Geochronological sample ESC-01 raises some interesting possibilities about the Taft Granite. It was taken from a large slab located out of the map area, ~125 m south of the start of *Zodiac* that was mapped by Calkins (1985) as Taft Granite. It petrographically resembles Taft Granite in hand sample, but cathodoluminescence on heavy minerals reveal the presence of monazite (A. Kylander-Clark, pers. comm., 2013). No petrographic description of the Taft Granite mentions monazite (Calkins, 1930; Pabst, 1938; Smith, 1967; Bateman et al., 1984; Ratajeski et al., 2001). This subtle difference suggests this rock may be a separate unit an idea that is supported by the laser date (106.6 ± 1.1). The Taft Granite contains cryptic contacts between temporally separate units with slight petrographic differences that are often interpreted as suggesting incremental assembly (Memeti et al., 2010; Coleman et al., 2012).

Tonalite of the Gray Bands

Because it is compositionally similar to the biotite-rich, hornblende-poor dikes of the Oceans, the tonalite of the Gray Bands has been interpreted as coeval mafic material that was mixed with the Taft Granite during emplacement (Ratajeski et al., 2001). However, in a few locations, such as at the lowest point of the bands, the tonalite of the Gray Bands cuts the

dikes of the Oceans, thus indicating they are separate intrusions and that the tonalite of the Gray Bands is younger. Furthermore, because the tonalite of the Gray Bands is only found in this one peripheral area of the Taft Granite and because it cross cuts the Taft Granite at the top of the North America Wall area, it must be interpreted as a separate intermediate intrusion rather than a ubiquitous marginal facies of a Taft Granite "magma chamber".

Because it has a gradational contact with the Taft above and sharp contact with the El Capitan below, the tonalite of the Gray Bands must have intruded along the contact of a thermally active Taft Granite and a cold, brittle El Capitan. Within the tonalite of the Gray Bands, there are large (up to ~20 m diameter) xenoliths of El Capitan Granite, but none of Taft. Perhaps this is because the tonalite of the Gray Bands, intruding into a cooler upper-crustal environment, would have cooled more rapidly at the roof and succeeding pulses of magma (indicated by the composite nature of the intrusion) would preferentially intrude at the base of prior intrusions (Leuthold et al., 2012). These units would have had more time to react with the El Capitan, generating the features interpreted as xenoliths.

Since the tonalite of the Gray Bands is unlike any other member of the ISYV, and intruded after what is recognized to be the latest stage of magmatism in the ISYV, it is perhaps a previously unrecognized marginal member of the intrusive suite of Buena Vista Crest. The intrusive suite of Buena Vista Crest has many mafic marginal members, including the Illilouette Creek and Tamarack Creek Granodiorites, the tonalite of Crane Creek, and the Leaning Tower Granite (Bateman 1992). The relation between and possible cogenesis of these units are very poorly understood. Given that the Leaning Tower Granite has been found in this area of the valley, it is not unreasonable to speculate that the tonalite of the Gray Bands could be one of the early-stage magmas of the intrusive suite of Buena Vista Crest.

33

Source of Aplites

Aplite magmas are late-stage melts from an evolving magma body and are commonly presumed to radiate outward during the final stages of pluton formation (Pitcher, 1997). The thin horizontal series of aplites on El Capitan can be seen on the north side of Yosemite Valley cutting all rocks until they reach the TIS. Because of these field relations, it is possible that they radiated out of the TIS and into the ~10 Ma older ISYV. This field relation has been observed in other plutons (Searle et al., 1993; Allibone et al., 2007).

However, aplite dikes in the ISYV do not display the low (<10 ppm) Y contents that are characteristic of aplites in the TIS (Glazner et al., 2008) but rather have concentrations similar to other aplites throughout the western United States (Figure 8B). The possibility that the dikes radiated outward from the TIS and assimilated Y from Y-normal country rocks is precluded by the fact that aplites throughout the ISYV are uniformly high in Y, even in rocks adjacent to the TIS (Figure 8C). This suggests that aplites cropping out on El Capitan formed in-situ, rather than radiating outward from the TIS as field relations would suggest.

Geomorphologic differences

The differences in morphology between the southeast and southwest faces of El Capitan indicate that the distribution of Cretaceous granitoids may have played a role in shaping the monolith. The southeast face overhangs up to ~35 m with a typical slope of -86° compared with the southwest face, which has a typical slope of 81°. This different morphology may, in part, be due to near-absence of mafic dikes on the southwest face compared to their ubiquitous presence on the southeast face. Mafic dikes have a greater abundance of weaker minerals, particularly biotite, resulting in a lower rock-mass strength

than the host granites. As has been observed in other studies (Schmidt and Montgomery, 1995; Korup, 2008), weaker rocks preferentially weather and provide surfaces from which jointing can propagate and can result in steeper slopes. We suggest that preferential weathering of mafic dikes may be the source of El Capitan's distinctive shape and perhaps even a contributing factor to the original incision of Yosemite Valley.

Vertical geochemistry

This study provided a rare opportunity to study compositional trends along the vertical dimension of a frozen magmatic system. Many hypotheses for the generation of silicic melts are based on gravitational separation of melt from crystals and predict upward accumulation of liquids rich in silica and incompatible elements (Baker and McBirney, 1985; Hildreth, 2004). Several studies inferring vertical zonation in silicic systems were not of true vertical transects, but rather inclined lines of sampling from which vertical variation was inferred, or subhorizontal transects of tilted plutons (Sawka et al., 1990; Verplanck et al., 1999; Bachl et al., 2001). These trends should be observable within the primary silicic units exposed by the southeast face of El Capitan.

There is no compositional trend with elevation in the whole-rock data within the El Capitan or the Taft Granites (Figure 10). If gravity-driven crystal/liquid separation within a shallow magma chamber was a significant process in formation of the compositional heterogeneity displayed on El Capitan, then one would expect to observe increasing SiO_2, K_2O, Al_2O_3 and decreasing $Fe_2O_3^t$, MgO, CaO and Na_2O within each unit as elevation increases.

There are also no vertical trends in the relative abundance and mean crystal size of feldspars and ferromagnesian minerals within the El Capitan Granite. Traditional models predict that the outer parts of the pluton, being the fastest cooling and most mafic, should have larger and more abundant ferromagnesian minerals. The rocks of the inner and structurally higher areas of a pluton should have larger K-feldspar crystals given their prolonged cooling times (Sawka et al., 1990; Verplanck et al., 1999; Economos et al., 2010). This heterogeneity in rock texture indicates the El Capitan Granite experienced a far more complex emplacement history during emplacement than fractional crystallization models would suggest.

Another line of evidence used to support ideas of crystal-liquid fractionation is the presence of modal layering, mafic banding, schlieren or leucocratic veins (Weinberg et al., 2001; Žák and Paterson 2006). These features are almost nonexistent in the El Capitan Granite. Although mafic bands and modal layering are locally present within the Taft Granite, they are rarely oriented parallel to the pluton walls. This is contrary to what traditional models predict in a tank of magma where modal layering can occur at the edges of solidification fronts migrating inward along a thermal gradient (Weinberg et al., 2001; Wyborn et al., 2001). Furthermore, Reid et al (1993) found that, in the Tuolumne Intrusive Suite, modal layering did not result in the suite-scale changes in geochemistry and therefore is not suggestive of crystal/liquid fractionation as a first-order process in pluton emplacement.

Recent studies (Clemens et al., 2010; Tappa et al., 2011; Coleman et al., 2012) suggest that compositional heterogeneity within intrusive suites and individual units is inherited from the source of a magma rather than produced by *in situ* crystal/liquid

fractionation. The vertical chemical and textural profiles within units on El Capitan may be accord with these studies. Whereas compositional heterogeneity may exist on a suite-wide scale, the El Capitan Granite is internally disordered, and the Taft Granite's variety can be explained by second-order processes such as crystal/liquid fractionation at meter scale. Because evidence of large scale differentiation is lacking in the vertical profiles of the rocks of El Capitan, we suggest the compositional heterogeneity of the ISYV is inherited from the source rather than shallow crustal processes.

CONCLUSIONS

New meter scale geologic mapping of El Capitan in Yosemite Valley, California reveals much about the complex emplacement history of this portion of the Sierra Nevada Batholith: 1) Eight distinct intrusive episodes of granitoids from the intrusive suites of Yosemite Valley and Buena Vista Crest were mapped and chronologically ordered using cross-cutting relations and geochronology. These episodes reflect an intrusive history that spans ~2.9 Ma and occurred under a variety of thermal and rheologic conditions. 2) Mafic dikes are dominantly distributed on the eastern portion of the face, and are hypothesized to be one of the reasons for El Capitan's distinctive shape. 3) Aplite dikes display geochemistry suggestive of local growth, calling into question the idea that they were injected laterally from the TIS. 4) Evidence of large-scale *in situ* crystal/liquid fractionation is conspicuously absent from the whole-rock compositions and petrographic textures of the dominant silicic units, suggesting lower crustal processes were the cause of compositional heterogeneity displayed on the face of El Capitan.

APPENDIX 1: TEXTURE PHOTOS AND SAMPLE LOCATIONS
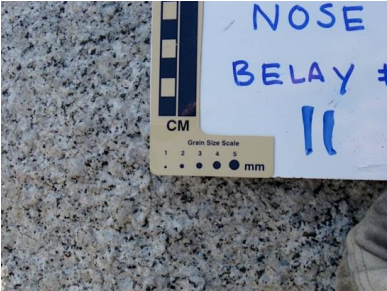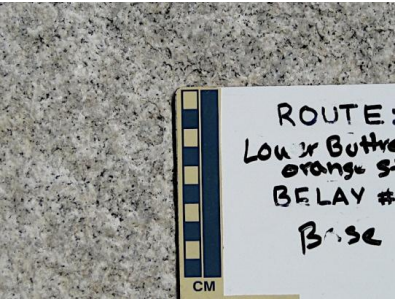
Locations of all scale photographs and samples taken on the southeast face over the course of this study.
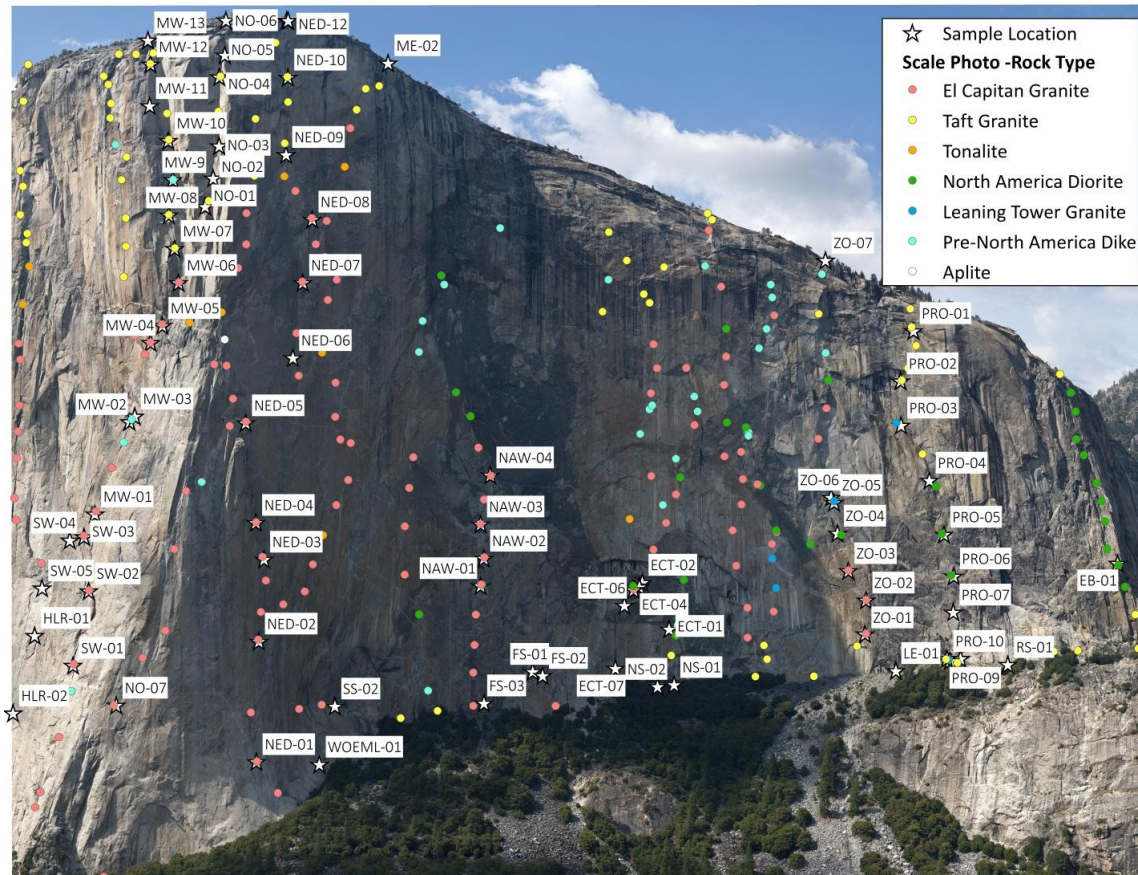
APPENDIX 2: SUMMARY OF PETROGRAPHY

Summary of the petrography of the units found on and around El Capitan drawn from this study and descriptions by

Calkins (1930), Pabst (1938), Smith (1967), and Ratajeski et al. (2001).

APPENDIX 2: SUMMARY OF PETROGRAPHY
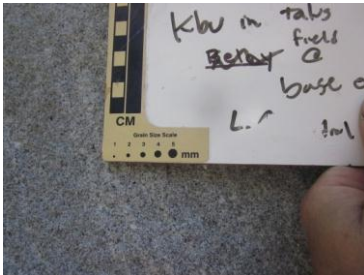
Unit	Age (Ma)*	Grain size	Megascopic features	Texture	Microscopic features	Acessory minerals	Texture photo
El Capitan Granite	115-105.7	Range 0.5-7 mm (occasional feldspar phenocrysts are at least 11 mm in diam.)	Light gray, medium to coarse-grained locally, finer-grained near western contact.	K-feldspar porphry	Antiperthitic plagioclase, poikilitic alkali fedspaer with strings of microperthite twinning. Anhedral, fractured quartz with pronounced wavy extinction. Biotite is common and hornblende is essentially absent.	Allanite, zircon, titanite, apatite	
Taft Granite	106-104	Range 1-3.5 mm, typically equigranular	Very light gray, medium-fine grained (resembles the El Capitan. but is finer grained and more uniform).	Hypidiomorphic granular	Abundant myrmekite. Plagioclase often enclosed in microperthite. Biotite average about 3 % by volume and is the only mafic constituant.	Zircon, allanite, apatite, ilmenite. Acessory minerals are rare.	

APPENDIX 2: SUMMARY OF PETROGRAPHY CONTD.

Unit	Age*	Grain size	Megascopic features	Texture	Microscopic features	Acessory minerals	Texture photo
Leaning Tower Granite	104.1	Range 0.5-3 mm. Mafic phenocrysts up to 5 mm	Medium-dark gray, medium-fine grained	Hypidiomorp-hic granular with distinctive clots of biotite 10 mm diameter	Perthitic feldspar, with moderately abundant myrmekite. Clusters of biotite and hornblende make up about 10% volume.	Acessory minerals abundant. Include magnetite, zircon, illmentie	
Tonalite of the gray Bands	ND	Range 0.5-3 mm	Medium-dark gray. Fine grained.	Hypidiomorp-hic granular with biotite foliation	Perthitic feldspar. Biotite commonly chloritized. Rare intergranular biotite within feldspars. Quartz exhibits patchy extinction.	Acessory minerals uncommon. Titanite, zircon, epidote.	
Dikes of the Oceans	ND	Range 0.5-3 mm	Medium-dark gray. Fine-medium grained.	Hypidiomorp-hic granular.	NA	NA	

APPENDIX 2: SUMMARY OF PETROGRAPHY CONTD.

Unit	Age*	Grain size	Megascopic features	Texture	Microscopic features	Acessory minerals	Texture photo
Diorite of North America	103	Range 0.5-3 mm. Occaisional horbnlende phenocrysts up to 10m common in dense aggregates	Dark gray to black. Fine-medium grained	Diverse. Typically hypidiomorp-hic granular	Compositionally diverse. Generally hornblende laths in a granular matrix consisting largly of plagioclase and quartz. Biotite poor. Plagioclase often have partially resorbed cores. Apatite exixts in elongate needles	Apatite, titanite, zircon, magnetite	
Bridalveil Granodiorite	103.5	Range 0.5-2 mm . Typically equigranular.	Medium-dark gray, darker than the Leaning Tower Granite. Very fine grained	Allotriomorp-hic granular	Feldspars commonly perthitic. Osciliatory zoning in plagioclase. Anhedral qurtz with patchy extinction. Myrmekite abundant. Rare hornblende	Zircon, magnetite, titanite, apatite, allanite, epidote, rare pyrite	
Aplite Dikes	ND	Range > 0.5 mm to 20 mm	White-light gray. Typically fine grained, though sometimes very coarse	Texturally diverse. Pegmatitic to aphanitic. Locally graphic	NA	Garnet, muscovite, allanite, epidote	

Note: If a feature is listed as "NA", it was not analyzed nor could it be found in the literature.
*All ages are from this study unless marked with a "ND" if the unit remains undated.

APPENDIX 3: WHOLE ROCK DATA

Sample number	Rock type	Relative elevation (m)*	SiO_2	TiO_2	Al_2O_3	$Fe_2O_3^T$	MnO	MgO	CaO	Na_2O	K_2O	P_2O_3	Sum	LOI	Location description*
EB-01	Kap	354	76.67	0.05	12.83	0.52	0.02	0.01	0.41	2.67	6.80	0.00	99.96	0.34	"The East Buttress of El Capitan", belay 4
ECT-01	Kt	272	75.94	0.09	13.06	1.23	0.04	0.14	1.08	2.96	5.35	0.02	99.91	0.23	"El Capitan Tree", belay 3
ECT-02	Kap	315	76.43	0.07	13.54	0.79	0.02	0.21	1.31	3.66	4.30	0.00	100.32	0.23	"El Capitan Tree", belay 5
ECT-04	Kec	308	75.07	0.29	13.69	2.51	0.05	0.71	3.29	3.83	1.01	0.04	100.49	0.38	"El Capitan Tree", belay 7
ECT-06	Kap	292	77.04	0.03	13.23	0.58	0.02	0.04	0.88	3.86	4.58	0.00	100.25	0.18	"El Capitan Tree", 20 m down the first rappel
ECT-07	Kec	230	75.75	0.09	13.39	1.02	0.03	0.09	1.10	3.51	4.71	0.00	99.66	0.04	"El Capitan Tree", 40 m down the second rappel
FS-01	Kap	224	74.77	0.03	14.46	0.72	0.02	0.03	0.91	3.61	5.96	0.00	100.49	0.21	The Footstool, left side of the summit
FS-02	Kt	222	75.40	0.09	13.62	0.92	0.03	0.08	0.93	3.08	5.76	0.00	99.88	0.14	The Footstool, 4 m below right side of summit
HLR-01	Kec	239	72.16	0.26	14.93	2.14	0.05	0.50	1.92	3.56	4.58	0.02	100.11	0.44	Heart Ledges Rappel Line, first rappel station
HLR-02	Kec	163	74.64	0.22	13.68	1.99	0.05	0.44	1.81	3.47	3.72	0.03	100.06	0.33	Heart Ledges Rappel Line, 3rd rappel station
LC-01	Klt	N.A	70.61	0.41	14.95	3.20	0.06	1.11	3.07	3.44	3.53	0.06	100.42	0.37	Lower Cathedral Rock, float 10 m downslope of "Jungle Boogie"

APPENDIX 3. WHOLE ROCK DATA (CONT.)

Sample number	Rock type	Relative elevation (m)*	SiO_2	TiO_2	Al_2O_3	$Fe_2O_3^T$	MnO	MgO	CaO	Na_2O	K_2O	P_2O_5	Sum	LOI	Location description*
LC-02	Klt	N.A	69.36	0.48	15.96	3.34	0.06	0.97	3.43	3.71	2.92	0.11	100.34	0.33	Lower Cathedral Rock, float 10 m downslope of "Jungle Boogie"
LC-05	Klt	N.A	69.18	0.41	15.39	3.27	0.06	1.02	3.02	3.25	3.88	0.06	99.55	0.53	Lower Cathedral Rock, start of "Overhang Bypass"
LC-06	Klt	N.A	69.43	0.44	15.07	3.81	0.08	1.17	3.11	3.41	3.52	0.06	100.11	0.40	Lower Cathedral Rock, 10 m right of "End of the Line"
LJ-01	Kec	94	71.67	0.21	14.91	1.99	0.06	0.45	1.89	3.79	4.38	0.02	99.37	0.27	Left side of the summit of "Little John"
ME-02	Kt	813	76.25	0.15	13.42	1.46	0.03	0.24	1.31	3.17	4.38	0.02	100.43	0.38	"Mescalito", belay 26
MW-01	Kec	360	72.00	0.30	15.14	2.42	0.05	0.65	2.25	3.58	4.00	0.05	100.43	0.52	""Muir Wall"", belay 12
MW-02	Kec	451	74.81	0.24	13.42	2.00	0.04	0.47	1.92	3.24	3.75	0.02	99.91	0.25	"Muir Wall", belay 15
MW-03	Ktn	457	67.18	0.60	16.65	4.37	0.09	1.08	3.47	4.26	2.57	0.13	100.41	0.50	"Muir Wall", belay 15
MW-04	Ktn	529	66.03	0.59	17.38	4.48	0.12	1.37	4.02	4.57	1.95	0.14	100.64	0.53	"Muir Wall", belay 18
MW-05	Kec	546	72.66	0.27	14.37	2.46	0.04	0.65	2.35	3.52	3.57	0.04	99.92	0.28	"Muir Wall", belay 19
MW-06	Ktn	589	61.25	0.78	19.34	5.30	0.06	1.81	5.80	4.13	1.90	0.21	100.58	0.58	"Muir Wall", belay 21
MW-07	Kec	628	73.85	0.18	14.36	1.70	0.04	0.41	2.03	3.70	3.93	0.02	100.23	0.29	"Muir Wall", belay 22

Sample number	Rock type	Relative elevation (m)*	SiO_2	TiO_2	Al_2O_3	$Fe_2O_3^T$	MnO	MgO	CaO	Na_2O	K_2O	P_2O_3	Sum	LOI	Location description*
MW-08	Kt	654	74.24	0.18	13.95	1.70	0.02	0.28	1.77	3.42	4.16	0.00	99.73	0.33	"Muir Wall", belay 23
MW-09	Kt	688	76.41	0.14	13.10	1.68	0.03	0.19	1.35	3.30	4.27	0.00	100.46	0.30	"Muir Wall", belay 24
MW-10	Kt	727	76.78	0.12	12.94	1.36	0.03	0.18	1.25	3.14	4.59	0.00	100.39	0.49	"Muir Wall", belay 27
MW-11	Kt	760	74.13	0.15	14.14	1.45	0.05	0.22	1.39	3.42	4.80	0.01	99.75	0.35	"Muir Wall"(left), left of route, 2 rappels below the last anchor
MW-12	Kt	800	75.15	0.13	13.20	1.39	0.03	0.16	1.16	3.20	4.74	0.00	99.14	0.24	"Muir Wall"(left), left of route, 1 rappell below the last anchor
MW-13	Kt	823	70.16	0.42	15.76	3.29	0.11	0.85	2.83	4.32	2.39	0.09	100.21	0.41	"Muir Wall", belay 32
NAW-01	Kec	307	74.66	0.18	13.84	1.74	0.04	0.42	1.94	3.63	3.60	0.03	100.09	0.31	"North America Wall", belay 4
NAW-02	Kec	333	71.95	0.27	15.00	2.46	0.07	0.66	2.03	3.65	4.45	0.04	100.56	0.26	"North America Wall", belay 5
NAW-03	Kec	366	73.88	0.30	13.51	2.66	0.05	0.71	2.24	3.32	3.27	0.04	99.99	0.25	"North America Wall", belay 6
NAW-04	Kec	415	70.78	0.28	15.38	2.50	0.04	0.65	2.50	3.46	4.24	0.05	99.88	0.44	"North America Wall", belay 8
NED-01	Kec	126	74.64	0.21	13.57	1.89	0.04	0.42	1.75	3.31	4.22	0.02	100.06	0.31	"New Dawn", belay 1
NED-02	Kec	244	76.06	0.24	12.06	2.19	0.06	0.50	0.74	2.13	6.14	0.03	100.15	0.31	"New Dawn", belay 4
NED-03	Kec	322	71.40	0.25	15.21	2.22	0.05	0.54	2.05	3.77	4.32	0.03	99.85	0.22	"New Dawn", belay 7

Sample number	Rock type	Relative elevation (m)*	SiO$_2$	TiO$_2$	Al$_2$O$_3$	Fe$_2$O$_3$^{T}	MnO	MgO	CaO	Na$_2$O	K$_2$O	P$_2$O$_3$	Sum	LOI	Location description*
NED-04	Kec	358	75.42	0.27	12.66	2.36	0.07	0.59	1.63	3.15	3.89	0.03	100.06	0.41	"New Dawn", belay 8
NED-05	Kec	455	72.09	0.23	14.38	2.14	0.06	0.48	1.84	3.71	4.12	0.03	99.06	0.19	"New Dawn", belay 11
NED-06	Kec	520	73.79	0.23	14.14	2.11	0.06	0.50	1.77	3.56	4.27	0.02	100.46	0.34	"New Dawn", 30 m above belay 15
NED-07	Kec	595	72.59	0.23	14.79	1.99	0.05	0.48	2.06	3.80	4.03	0.03	100.06	0.53	"New Dawn", belay 17
NED-08	Kec	657	74.26	0.25	13.78	2.27	0.07	0.57	1.99	3.70	3.59	0.03	100.51	0.22	"New Dawn", belay 19
NED-09	Kt	718	75.99	0.14	13.01	1.46	0.02	0.20	1.39	3.30	4.33	0.00	99.83	0.36	"New Dawn", belay 22
NED-10	Kt	793	76.40	0.14	13.22	1.30	0.03	0.19	1.48	3.29	4.25	0.00	100.29	0.32	"New Dawn", belay 25
NED-12	Kt	852	70.47	0.11	12.32	1.29	0.03	0.17	1.05	2.96	4.34	0.02	92.75	0.40	"New Dawn", belay 28
NO-01	Kt	665	74.97	0.15	13.71	1.58	0.04	0.24	1.38	3.49	4.37	0.00	99.91	0.13	"The Nose", belay 24
NO-02	Kt	629	75.39	0.15	13.37	1.53	0.04	0.26	1.41	3.29	4.38	0.01	99.82	0.30	"The Nose", belay 25
NO-03	Kt	724	76.05	0.12	12.99	1.20	0.03	0.16	1.41	3.13	4.14	0.00	99.22	0.35	"The Nose", belay 26
NO-04	Kt	791	76.38	0.13	13.12	1.45	0.03	0.20	1.27	3.31	4.41	0.00	100.29	0.28	"The Nose", 10 m below belay 28
NO-05	Kt	812	72.52	0.28	14.62	2.56	0.07	0.55	2.19	4.23	2.78	0.05	99.85	0.26	"The Nose", belay 29
NO-06	Kt	847	75.73	0.12	13.49	1.30	0.03	0.16	1.11	3.03	5.18	0.00	100.13	0.53	"The Nose", belay 31
NO-07	Kec	175	73.78	0.19	13.93	1.89	0.05	0.42	1.77	3.49	4.20	0.02	99.73	0.21	"The Nose", belay 4

Sample number	Rock type	Relative elevation (m)*	SiO_2	TiO_2	Al_2O_3	$Fe_2O_3^T$	MnO	MgO	CaO	Na_2O	K_2O	P_2O_3	Sum	LOI	Location description*
NS-01	Klt	217	68.30	0.57	15.03	4.10	0.08	1.53	3.64	3.25	3.39	0.09	99.98	0.50	"Native Son", start of the route
PRO-01	Kt	572	75.83	0.07	13.26	0.95	0.03	0.09	1.00	2.81	5.87	0.00	99.89	0.18	"The Prophet", belay 14
PRO-02	Kt	523	76.78	0.11	12.86	1.34	0.02	0.13	1.33	2.73	5.06	0.00	100.33	0.70	"The Prophet", belay 9
PRO-03	Kt	479	77.97	0.11	12.01	1.43	0.04	0.13	1.08	2.71	4.70	0.00	100.18	0.64	"The Prophet", 1 m below belay 7
PRO-04	Kt	428	75.64	0.08	13.77	1.09	0.03	0.10	1.14	3.13	5.51	0.00	100.49	0.24	"The Prophet", 20 m above belay 5
PRO-06	Kap	335	76.18	0.02	13.50	0.45	0.02	0.00	0.68	3.34	5.85	0.00	100.02	0.29	"The Prophet", belay 3
PRO-07	Kt	301	75.58	0.13	13.14	1.37	0.03	0.18	1.33	3.00	4.87	0.00	99.62	0.43	"The Prophet", 25 m above belay 2
PRO-09	Klt	242	67.83	0.59	15.27	4.33	0.08	1.66	3.81	3.46	2.91	0.13	100.07	0.45	"The Prophet", start of the route
PRO-10	Kt	243	75.96	0.15	12.95	1.29	0.03	0.19	1.29	2.93	4.82	0.03	99.63	0.44	"The Prophet", 10 m right of the start of the route
SW-01	Kec	213	73.52	0.21	14.16	1.92	0.05	0.44	1.67	3.28	4.78	0.02	100.05	0.67	"Salathe Wall", belay 6
SW-02	Kec	285	74.20	0.19	13.80	1.87	0.05	0.45	1.91	3.50	3.70	0.02	99.67	0.32	"Salathe Wall", belay 8
SW-03	Kap	338	75.76	0.09	13.63	1.11	0.04	0.15	1.18	3.47	4.74	0.00	100.16	0.29	"Salathe Wall", belay 10
SW-04	Kec	334	74.63	0.20	13.99	1.73	0.05	0.39	1.71	3.42	4.35	0.02	100.48	0.25	"Salathe Wall", belay 10
SW-05	Kec	287	72.79	0.28	14.43	2.42	0.06	0.63	1.95	3.52	4.03	0.04	100.14	0.39	"Salathe Wall", belay 11
ZO-01	Kec	277	76.22	0.12	13.16	1.31	0.04	0.30	1.26	3.28	4.45	0.04	100.20	0.35	"Zodiac", belay 2
ZO-02	Kec	309	76.51	0.13	12.78	1.33	0.04	0.18	1.10	3.02	4.76	0.03	99.87	0.15	"Zodiac", belay 3

Sample number	Rock type	Relative elevation (m)*	SiO_2	TiO_2	Al_2O_3	$Fe_2O_3^T$	MnO	MgO	CaO	Na_2O	K_2O	P_2O_5	Sum	LOI	Location description*
ZO-03	Kt	337	75.63	0.12	13.51	1.22	0.04	0.14	1.12	3.23	5.08	0.02	100.11	0.22	"Zodiac", belay 4
ZO-06	Klt	410	68.43	0.54	15.26	3.97	0.07	1.49	3.71	3.33	2.92	0.12	99.85	0.44	"Zodiac", 10 m above belay 7
ZO-07	Kt	637	76.00	0.13	13.15	1.28	0.02	0.15	1.09	2.80	5.04	0.02	99.68	0.53	"Zodiac", belay 15

Note: Element compositions are in weight percent. Major element compositions express total Fe as Fe_2O_3 and have been normalized 100 wt% anhydrous. LOI—loss on ignition (in wt%).

*Most samples were taken from the face of >500m cliffs, rendering GPS readings useless. Therefore, locations are described relative to climbing routes fom McNamera and VanLueven (2011). Directions are in reference to the observer facing the cliff.

APPENDIX 4: APLITE TRACE-ELEMENT DATA

Sample number	Host rock	Ba	Rb	Sr	Y	Zr	Ni	Nb	Th	Cr	Cu	Zn	Location description*
BRO-01	Ks	78.67	169.01	87.82	2.54	26.80	0.00	0.90	17.80	69.30	2.00	12.40	Lower Brother, 30 m right of "Positively 4th Street"
BRO-02	Khd	76.66	134.68	82.29	1.74	22.90	0.80	0.00	17.60	136.20	2.00	15.90	10 m right of "Rixon's Pinnacle Right"
EB-01	Kd	2.07	319.89	10.41	7.21	12.40	3.20	4.80	10.40	95.50	0.70	13.50	"The East Buttress of El Capitan", belay 4
ECT-02	Kd	472.31	90.77	124.81	17.21	60.90	0.80	10.80	8.00	51.50	0.80	15.50	"El Capitan Tree", belay 5
ECT-06	Kd	345.81	113.33	80.23	15.92	27.50	0.00	13.80	5.80	68.20	0.00	15.40	"El Capitan Tree", 20 m down the first rappell
EGP-01	Kec	1212.24	170.67	187.65	26.52	25.40	1.70	31.40	6.10	0.00	0.80	10.00	269280, 4181129
EGP-02	Kec	240.73	92.72	92.20	9.48	36.30	0.00	11.80	26.00	65.80	1.40	11.90	268756, 4180619
EL-01	Kec	13.25	177.29	12.06	6.81	107.90	0.10	0.00	34.60	65.20	0.30	20.80	East Ledges Decent, first rappell station
EL-02	Kec	33.80	187.51	40.21	3.34	23.20	1.30	0.00	32.60	80.50	0.60	14.80	East Ledges Decent, 20 m left of the third rappell
FS-01	Kt	261.60	129.14	76.21	14.51	23.00	4.20	7.50	5.30	286.20	0.00	12.50	The Footstool, left side of the summit
FS-03	Kt	448.29	130.95	91.22	12.42	33.20	1.80	14.60	7.50	114.00	4.90	19.60	3 m up "Wyoming Sheep Ranch"
FT-01	Kec	49.87	164.23	21.42	32.65	39.50	3.10	14.00	32.30	130.50	2.70	10.80	271045, 4181409
FT-02	Kec	512.24	146.20	107.58	22.81	101.20	2.60	9.80	45.00	76.80	3.10	11.30	270765, 4181945

Sample number	Host rock	Ba	Rb	Sr	Y	Zr	Ni	Nb	Th	Cr	Cu	Zn	Location description*
FT-03	Kec	58.52	152.03	23.89	20.54	28.60	3.20	15.40	29.70	93.70	6.70	11.50	271047, 4182592
FT-04	Kec	96.72	140.68	39.44	6.83	0.00	1.10	4.10	13.10	75.40	1.00	10.60	270861, 4183146
LE-01	Kt	596.27	147.53	84.94	12.14	39.30	0.30	22.00	6.10	13.10	0.90	23.00	Start of "Lunar Eclipse"
ME-01	Kt	114.37	125.04	59.74	9.08	17.20	0.30	7.10	10.40	71.50	0.00	10.30	"Mescalito", belay 26
NED-11	Kt	168.07	126.82	56.40	22.74	34.30	0.90	15.20	9.20	43.10	1.40	13.60	"New Dawn" belay 28
NF-01	Khd	184.52	165.73	121.98	2.13	55.30	0.00	0.00	20.20	73.40	5.90	10.80	216136, 4178441
NS-02	Klt	252.39	159.96	50.73	16.02	26.80	0.70	12.50	6.20	50.90	2.80	19.30	10 m left of the start of the route
PRO-06	Kt	20.35	305.19	9.27	6.58	27.20	3.30	2.20	9.40	89.80	0.00	15.30	The Prophet, belay 3
PRO-08	Kt	284.04	135.72	59.86	17.22	28.60	1.40	9.70	8.60	54.30	1.40	19.70	40 m right of the start of "The Prophet"
RA-01	Khd	395.19	180.20	223.20	3.12	32.70	1.70	2.00	19.30	64.20	1.80	19.80	"The Royal Arches" , belay 7
RA-02	Khd	400.57	172.88	225.37	3.89	35.80	0.80	0.80	16.80	40.90	4.90	20.50	"The Royal Arches" , belay 9
RA-03	Khd	575.32	169.66	227.87	1.88	31.90	1.30	0.00	16.70	51.10	2.90	17.00	274008, 4181083
RA-04	Khd	34.96	277.34	39.94	3.63	27.80	1.70	1.50	21.40	106.40	5.70	17.90	274737, 4181089
RHO-01	Kgp	93.74	165.08	85.77	2.49	30.00	0.40	3.00	18.50	89.10	19.90	10.70	30 m right of the summit of the talus below the Rhombus Wall
RS-01	Kt	464.76	147.60	82.18	18.02	51.20	1.50	15.80	11.90	71.80	0.10	21.60	20 m left of large rust streak at the start of "The Waterfall Route"

APPENDIX 3. APLITE TRACE ELEMENTS (CONT.)

Sample number	Host rock	Ba	Rb	Sr	Y	Zr	Ni	Nb	Th	Cr	Cu	Zn	Location description*
SS-02	Kec	751.49	159.62	147.01	16.57	66.10	1.90	18.90	8.10	47.60	4.60	21.80	Start of "South Seas"
SW-03	Kec	1083.92	105.95	204.69	10.98	72.00	0.20	15.60	8.40	4.30	0.00	32.80	Salathe Wall, belay 10
WOEML-01	Kec	260.38	85.68	96.64	7.79	18.10	0.30	3.90	20.20	61.70	0.90	15.20	10m up "The Wall of Early Morning Light"
ZO-04	Kd	83.15	429.69	28.42	52.45	87.00	6.60	23.20	18.20	45.80	0.00	8.40	"Zodiac", belay 6
ZO-05	Kd	4.09	345.88	0.00	35.83	95.50	4.10	16.20	20.60	76.80	1.80	19.80	"Zodiac", belay 7

Note: Samples stored in the collections of University of North Carolina, Chapel Hill Department of Geological Sciences, Chapel Hill, North Carolina 27599. Trace element compositions in parts per million.

*Most samples were taken from the face of >500m cliffs, rendering GPS readings useless. Therefore, locations are described in reference to climbing routes fom McNamera and VanLueven (2011) or Reed (1996). Directions are in reference to the observer facing the cliff. UTM's given are in NAD 1983, Zone 11N.

REFERENCES

Allibone, A.H., Turnbull, I.M., Tulloch, A.J., and Cooper, A.F., 2007, Plutonic rocks of the Median Batholith in southwest Fiordland, New Zealand: field relations, geochemistry, and correlation: New Zealand Journal of Geology and Geophysics, v. 50, no. 4, p. 283–314.

Bachl, C.A., Miller, C.F., Miller, J.S., and Faulds, J.E., 2001, Construction of a pluton: Evidence from an exposed cross section of the Searchlight pluton, Eldorado Mountains, Nevada: Geological Society of America Bulletin, v. 113, no. 9, p. 1213–1228, doi: 10.1130/0016-7606(2001)113<1213:COAPEF>2.0.CO;2.

Bachmann, O., Dungan, M.A., and Lipman, P.W., 2002, The Fish Canyon magma body , San Juan Volcanic Field , Colorado : Rejuvenation and eruption of an upper-crustal batholith: Journal of Petrology, v. 43, no. 8, p. 1469–1503.

Bacon, C.R., and Druitt, T.H., 1988, Compositional evolution of the zoned calcalkaline magma chamber of Mount Mazama, Crater Lake, Oregon: Contributions to Mineralogy and Petrology, v. 98, no. 2, p. 224–256.

Baker, B.H., and McBirney, A.R., 1985, Liquid fractionation. Part III: Geochemistry of zoned magmas and the compositional effects of liquid fractionation: Journal of Volcanology and Geothermal Research, v. 24, p. 55–81.

Bartley, J.M., Coleman, D.S., and Glazner, A.F., 2008, Incremental pluton emplacement by magmatic crack-seal: Transactions of the Royal Society of Edinburgh–Earth Sciences, v. 97, no. for 2006, p. 383–396.

Bateman, P.C., and Chappell, B.W., 1979, Crystallization, fractionation, and solidification of the Tuolumne Intrusive Series, Yosemite National Park, California: Bulletin of the Geological Society of America, v. 90, no. 5, p. 465-482.

Bateman, P.C., Dodge, F.C.W., and Bruggman, P.E., 1984, Major oxide analyses, CIPW norms, modes and bulk specific gravities of plutonic rocks from the Mariposa 1° by 2° sheet, central Sierra Nevada, California: U.S. Geological Survey Open File Report, p. 84-162.

Bateman, P.C., 1992, Plutonism in the central part of the Sierra Nevada batholith, California: U.S. Geological Survey Professional Paper, v. 1483, 186 p.

Bowring, J.F., McLean, N.M., and Bowring, S.A., 2011, Engineering cyber infrastructure for U-Pb geochronology: Tripoli and U-Pb_Redux: Geochemistry Geophysics Geosystems, v. 12, p. Q0AA19, doi:10.1029/2010GC003479.

Buddington, A. F., 1959, Granite emplacement with special reference to North America: Geological Society of America Bulletin, v. 70, p. 671-747.

Calkins, F.C., 1930, The granitic rocks of the Yosemite region: U.S. Geological Survey Professional Paper, v. 160, p. 120-129.

Calkins, F.C., 1985, Bedrock geologic map of Yosemite Valley, Yosemite National Park, California: U.S. Geological Survey Map I-1639, scale 1:24,000.

Clemens, J.D., Helps, P. A., and Stevens, G., 2010, Chemical structure in granitic magmas – a signal from the source?: Earth and Environmental Science Transactions of the Royal Society of Edinburgh, v. 100, no. 1-2, p. 159–172, doi: 10.1017/S1755691009016053.

Coleman, D.S., Gray, W., and Glazner, A.F., 2004, Rethinking the emplacement and evolution of zoned plutons: Geochronologic evidence for incremental assembly of the Tuolumne Intrusive Suite, California: Geology, v. 32, no. 5, p. 433-436, doi: 10.1130/G20220.1.

Coleman, D. S., Bartley, J.M., Glazner, A.F., and Pardue, M.J., 2012, Is chemical zonation in plutonic rocks driven by changes in source magma composition or shallow-crustal differentiation?: Geosphere, v. 8, no. 6, p. 1568-1587. doi:10.1130/GES00798.1.

Coombs, M.L., and Gardner, J.E., 2001, Shallow-storage conditions for the rhyolite of the 1912 eruption at Novarupta, Alaska: Geology, v. 29, no. 9, p. 775-778, doi: 10.1130/0091-7613(2001)029<0775:SSCFTR>2.0.CO;2.

Daly, R.A., 1933, Igneous Rocks and the depths of the Earth: McGraw Hill, New York, NY, 598 p.

Davis, J.W., Coleman, D.S., Gracely, J.T., Gaschnig, R., and Stearns, M., 2011, Magma accumulation rates and thermal histories of plutons of the Sierra Nevada batholith, CA: Contributions to Mineralogy and Petrology, v. 163, no 3, p. 449-465: doi: 10.1007/s00410-011-0683-7.

Deering, C.D., Bachmann, O., and Vogel, T. A., 2011, The Ammonia Tanks Tuff: Erupting a melt-rich rhyolite cap and its remobilized crystal cumulate: Earth and Planetary Science Letters, v. 310, no. 3-4, p. 518–525, doi: 10.1016/j.epsl.2011.08.032.

Economos, R.C., Memeti, V., Paterson, S.R., Miller, J.S., Erdmann, S., and Žák, J., 2010, Causes of compositional diversity in a lobe of the Half Dome granodiorite, Tuolumne Batholith, Central Sierra Nevada, California: Earth and Environmental Science Transactions of the Royal Society of Edinburgh, v. 100, no. 1-2, p. 173–183, doi: 10.1017/S1755691009016065.

Eichelberger, J.C., Chertkoff, D.G., Dreher, S.T., and Nye, C.J., 2000, Magmas in collision: Rethinking chemical zonation in silicic magmas: Geology, v. 28, no. 7, p. 603–606.

Glazner, A.F., Bartley, J.M., Coleman, D.S., Gray, W., and Taylor, R.Z., 2004, Are plutons assembled over millions of years by amalgamation from small magma chambers?: GSA Today, v. 14, p. 4–12, doi: 10.1130/1052-5173(2004)014<0004.

Glazner, A.F., Coleman, D.S., and Bartley, J.M., 2008, The tenuous connection between high-silica rhyolites and granodiorite plutons: Geology, v. 36, no. 2, p. 183-186, doi: 10.1130/G24496A.1.

Gray, W., Glazner, A. F., Coleman, D.S., and Bartley, J.M., 2008, Long-term geochemical variability of the Late Cretaceous Tuolumne Intrusive Suite, central Sierra Nevada, California: Geological Society of London, Special Publications, v. 304, p. 183–201, doi: 10.1144/SP304.10.

Hildreth, W., 2004, Volcanological perspectives on Long Valley, Mammoth Mountain, and Mono Craters: several contiguous but discrete systems: Journal of Volcanology and Geothermal Research, v. 136, no. 3-4, p. 169–198, doi: 10.1016/j.jvolgeores.2004.05.019.

Huber, N.K., ,Bateman, P.C., and Wahrhaftig, C., 1989, Geologic map of Yosemite National Park and vicinity, California: U.S. Geological Survey, Miscellaneous Investigations Map I-1874, scale 1:125,000.

Ingalls, M., 2011, A study of the temporal evolution of the El Capitan Granite using high-precision U-Pb zircon geochronology [Honors thesis]: Chapel Hill, University of North Carolina at Chapel Hill, 24 p.

Korup, O., 2008, Rock type leaves topographic signature in landslide-dominated mountain ranges: Geophysical Research Letters, v. 35, no. 11, p. L11402, doi: 10.1029/2008GL034157.

Krogh, T.E., 1973, A low-contamination method for hydrothermal decomposition of zircon and extraction of U and Pb for isotopic age determinations: Geochimica Cosmochimica Acta, v. 37, p. 485-494.

Kylander-Clark, A.R.C., Hacker, B.R., and Cottle, J.M., 2013, Laser-ablation split-stream ICP petrochronology: Chemical Geology, v. 345, p. 99–112, doi: 10.1016/j.chemgeo.2013.02.019.

Leuthold, J., Müntener, O., Baumgartner, L.P., Putlitz, B., Ovtcharova, M., and Schaltegger, U., 2012, Time resolved construction of a bimodal laccolith (Torres del Paine, Patagonia): Earth and Planetary Science Letters, v. 325-326, p. 85–92, doi: 10.1016/j.epsl.2012.01.032.

Mattinson, J.M., 2005, Zircon U-Pb chemical abrasion (“CA-TIMS”) method: Combined annealing and multi-step partial dissolution analysis for improved precision and accuracy of zircon ages: Chemical Geology v. 220 p. 47-66.

Matzel, J.E.P., Bowring, S. a., and Miller, R.B., 2006, Time scales of pluton construction at differing crustal levels: Examples from the Mount Stuart and Tenpeak intrusions, North

Cascades, Washington: Geological Society of America Bulletin, v. 118, no. 11-12, p. 1412–1430, doi: 10.1130/B25923.1.

McLean, N.M., Bowring, J.F., and Bowring, S.A., 2011, An algorithm for U-Pb isotope dilution data reduction and uncertainty propagation, Geochemistry Geophysics Geosystems, v. 12, p. Q0AA18, doi:10.1029/2010GC003478.

McNamara, C., Van Leuven, C., 2011, Yosemite Big Walls, Third Edition: Mill Valley, CA, SuperTopo, 208 p.

Memeti, V., Paterson, S., Matzel, J., Mundil, R., and Okaya, D., 2010, Magmatic lobes as "snapshots" of magma chamber growth and evolution in large, composite batholiths: An example from the Tuolumne intrusion, Sierra Nevada, California: Geological Society of America Bulletin, v. 122, no. 11-12, p. 1912–1931, doi: 10.1130/B30004.1.

Michel, J., Baumgartner, L., Putlitz, B., Schaltegger, U., and Ovtcharova, M., 2008, Incremental growth of the Patagonian Torres del Paine laccolith over 90 k.y: Geology, v. 36, no. 6, p. 459-462, doi: 10.1130/G24546A.1.

Miller, C.F., and Miller, J.S., 2002, Contrasting stratified plutons exposed in tilt blocks, Eldorado Mountains, Colorado River Rift, NV, USA: Lithos, v. 61, no. 3-4, p. 209–224, doi: 10.1016/S0024-4937(02)00080-4.

Miller, R.B., and Paterson, S.R., 1999, In defense of magmatic diapirs: Journal of Structural Geology, v. 21, no. 8-9, p. 1161–1173, doi: 10.1016/S0191-8141(99)00033-4.

Nelson, W.R., Dorais, M.J., Christiansen, E.H., and Hart, G.L., 2012, Petrogenesis of Sierra Nevada plutons inferred from the Sr, Nd, and O isotopic signatures of mafic igneous complexes in Yosemite Valley, California: Contributions to Mineralogy and Petrology, v. 165, no.2, p. 397-417, doi: 10.1007/s00410-012-0814-9.

Pabst, A.L., 1938, Heavy minerals in the granitic rocks of the Yosemite region: The American Mineralogist v. 23, p. 46-53.

Parrish, R.R., 1987, An improved micro-capsule for zircon dissolution in U-Pb geochronology: Chemical Geology, v. 66, p. 99-102.

Parrish R.R., and Krogh T.E., 1987, Synthesis and purification of [205]Pb for U-Pb geochronology: Chemical Geology v. 66, p. 103-110.

Peck, D. L., 2002, Geologic map of the Yosemite Quadrangle, central Sierra Nevada, California: U.S. Geological Survey Map I-2751, scale 1:62,500.

Pitcher, W.S., 1997, The Nature and Origin of Granite: 2nd edition, Chapman and Hall, New York, 387 p.

Ratajeski, K., Glazner, A.F., and Miller, B.V., 2001, Geology and geochemistry of mafic to felsic plutonic rocks in the Cretaceous intrusive suite of Yosemite Valley, California: Geological Society of America Bulletin, v. 113, no. 11, p. 1486-1502.

Ratajeski, K., Sisson, T.W., and Glazner, A.F., 2005, Experimental and geochemical evidence for derivation of the El Capitan Granite, California, by partial melting of hydrous gabbroic lower crust: Contributions to Mineralogy and Petrology, v. 149, no. 6, p. 713–734, doi: 10.1007/s00410-005-0677-4.

Reed, D., 1998, Yosemite Valley Free Climbs, Second Edition: Guilford, CT, The Globe Pequot Press, 423 p.

Reid J.B., Jr., Evans, O.C., and Fates, D.G., 1983, Magma mixing in granitic rocks of the central Sierra Nevada, California: Earth and Planetary Science Letters, v. 66, p. 243–261.

Reid, J. B., Jr., Murray, D., Hermes, O., and Steig, E., 1993, Fractional crystallization in granites of the Sierra Nevada: How important is it?: Geology, v. 21, no. July, p. 587–590.

Sawka, W., Chappell, B., and Kistler, R., 1990, Granitoid compositional zoning by side-wall boundary layer differentiation: evidence from the Palisade Crest Intrusive Suite, central Sierra Nevada, California: Journal of Petrology, v. 31, no. 3, p. 519-553.

Schmidt, K.M., and Montgomery, D.R., 1995, Limits to relief: Science, v. 270, no. 5236, p. 617–620.

Schmitz, M.D., and Bowring, S.A., 2001, U-Pb zircon and titanite systematics of the Fish Canyon Tuff: an assessment of high-precision U-Pb geochronology and its application to young volcanic rocks: Geochimica et Cosmochimica Acta, v. 65, no. 15, p. 2571–2587.

Searle, M.P., Metcalfe, R.P., Rex, A.J., and Norry, M.J., 1993, Field relations, petrogenesis and emplacement of the Bhagirathi leucogranite, Garhwal Himalaya: Geological Society Special Publication, no. 74, p. 429–444.

Smith, A. R., 1967, Petrography of six granitic intrusive units in the Yosemite Valley area, California: California Division of Mines Special Report, v. 91, p. 3-15

Steiger, R.H., and Jäger, E., 1977, Subcommission on geochronology: Convention on the use of decay constants in geo- and cosmochronology: Earth and Planetary Science Letters, v. 36, p. 359-362.

Stern, T.W., Bateman, P.C., Morgan, B.A., Newell, M.F., and Peck, D.L., 1981, Isotopic U-Pb ages of zircon from the granitoids of the central Sierra Nevada, California: US Geological Survey Professional Paper 1185, 17 p.

Stock, G.M., and Uhrhammer, R.A., 2010, Catastrophic rock avalanche 3600 years BP from El Capitan, Yosemite Valley, California: Earth Surface Processes and Landforms, v. 35, no. 8, p. 941–951, doi:10.1002/esp.1982.

Tappa, M.J., Coleman, D.S., Mills, R.D., and Samperton, K.M., 2011, The plutonic record of a silicic ignimbrite from the Latir volcanic field, New Mexico: Geochemistry Geophysics Geosystems, v. 12, no. 10, p. 1–16, doi: 10.1029/2011GC003700.

Tobisch, O.T., Saleeby, J.B., Renne, P.R., McNulty, B., and Tong, W., 1995, Variations in deformation fields during development of a large-volume magmatic arc, central Sierra Nevada, California: GSA Bulletin, v. 107, no. 2, p. 148–166.

Turner, S., Sandiford, M., Reagan, M., Hawkesworth, C., and Hildreth, W., 2010, Origins of large-volume, compositionally zoned volcanic eruptions: New constraints from U-series isotopes and numerical thermal modeling for the 1912 Katmai-Novarupta eruption: Journal of Geophysical Research, v. 115, B12201, doi: 10.1029/2009JB007195.

Verplanck, P.L., Farmer, G.L., McCurry, M., and Mertzman, S.A., 1999, The chemical and isotopic differentiation of an epizonal magma body: Organ Needle Pluton, New Mexico: Journal of Petrology, v. 40, no. 4, p. 653-678.

Weinberg, R.F., Sial, A. N., and Pessoa, R.R., 2001, Magma flow within the Tavares pluton, northeastern Brazil: Compositional and thermal convection: Geological Society of America Bulletin, v. 113, no. 4, p. 508–520, doi: 10.1130/0016-7606(2001)113<0508:MFWTTP>2.0.CO;2.

Wiebe, R.., and Collins, W.., 1998, Depositional features and stratigraphic sections in granitic plutons: implications for the emplacement and crystallization of granitic magma: Journal of Structural Geology, v. 20, no. 9-10, p. 1273–1289, doi: 10.1016/S0191-8141(98)00059-5.

Wyborn, D., Chappell, B.W., and James, M., 2001, Examples of convective fractionation in high-temperature granites from the Lachlan Fold Belt: Australian Journal of Earth Sciences, v. 48, no. 4, p. 531–541, doi: 10.1046/j.1440-0952.2001.00877.x.

Žák, J., and Paterson, S.R., 2005, Characteristics of internal contacts in the Tuolumne Batholith, central Sierra Nevada, California (USA): Implications for episodic emplacement and physical processes in a continental arc magma chamber: Geological Society of America Bulletin, v. 117, no. 9, p. 1242–1255, doi: 10.1130/B25558.1.